FOREWORD

This work was conducted by the National Carbon Company, a Division of Union Carbide Corporation, under USAF Contract AF 33(616)-6915. This contract was initiated under Project No. 7350 "Refractory Inorganic Non-Metallic Materials," Task No. 735002 "Refractory Inorganic Non-Metallic Materials: Graphitic;" Project No. 7381 "Materials Application," Task No. 738102 "Materials Process;" and Project No. 7-817 "Process Development for Graphite Materials." The work was administrated under the direction of the AF Materials Laboratory, Aeronautical Systems Division, with Captain R. H. Wilson, L. J. Conlon and W. P. Conrardy acting as Project Engineers.

Work under this contract has been in progress since May 1, 1960. The work covered in this report was conducted at the Research Laboratory of the National Carbon Company located at Parma 30, Ohio, under the direction of J. C. Bowman, Director of Research, and W. P. Eatherly, Assistant Director of Research.

The authors would like to thank Dr. H. J. Bowlden and Mrs. L. B. Smith for programming and carrying out the computer calculations given in Appendix II. Helpful discussions with Dr. J. N. Pike and Dr. R. G. Lye on the analysis of thermal conduction are gratefully acknowledged.

Prior reports issued under USAF Contract AF 33(616)-6915 have included:

WADD Technical Notes 61-18 and 61-18, Part II, progress reports covering work from the start of the Contract on May 1, 1960 to October 15, 1961, and the following volumes of WADD Technical Report 61-72 covering various subject phases of the work:

Volume I	Observations by Electron Microscopy of Dislocations in Graphite, by R. Sprague.
Volume II	Applications of Anisotropic Elastic Continuum Theory to Dislocations in Graphite, by G. B. Spence.
Volume III	Decoration of Dislocations and Low Angle Grain Boundaries in Graphite Single Crystals, by R. Bacon and R. Sprague.
Volume IV	Adaptation of Radiographic Principles to the Quality Control of Graphite, by R. W. Wallouch.
Volume V	Analysis of Creep and Recovery Curves for ATJ Graphite, by E. J. Seldin and R. N. Draper.
Volume VI	Creep of Carbons and Graphites in Flexure at High Temperatures, by E. J. Seldin.
Volume VII	High Density Recrystallized Graphite by Hot Forming, by E. A. Neel, A. A. Kellar, and K. J. Zeitsch.

Volume VII Supplement	High Density Recrystallized Graphite by Hot Forming, by G. L. Rowe and M. B. Carter.
Volume VIII	Electron Spin Resonance in Polycrystalline Graphite, by L. S. Singer and G. Wagoner.
Volume IX	Fabrication and Properties of Carbonized Cloth Composites, by W. C. Beasley and E. L. Piper.
Volume X	Thermal Reactivity of Aromatic Hydrocarbons, by I. C. Lewis and T. Edstrom.
Volume X Supplement	Thermal Reactivity of Aromatic Hydrocarbons, by I. C. Lewis and T. Edstrom.
Volume XI	Characterization of Binders Used in the Fabrication of Graphite Bodies, by E. de Ruiter, A. Halleux, V. Sandor, H. Tschamler.
Volume XI Supplement	Characterization of Binders Used in the Fabrication of Graphite Bodies, by E. de Ruiter, J. F. M. Oth, V. Sandor, and H. Tschamler.
Volume XII	Development of an Improved Large Diameter Fine Grain Graphite for Aerospace Applications, by C. W. Waters and E. L. Piper.
Volume XII Supplement	Development of an Improved Large Diameter Fine Grain Graphite for Aerospace Applications, by R. L. Racicot and C. W. Waters.
Volume XIII	Development of a Fine-Grain Isotropic Graphite for Structural and Substrate Applications, by R. A. Howard and E. L. Piper.
Volume XIII Supplement	Development of a Fine-Grain Isotropic Graphite for Structural and Substrate Applications, by R. A. Howard and R. L. Racicot.
Volume XIV	Study of High Temperature Tensile Properties of ZTA Grade Graphite, by R. M. Hale and W. M. Fassell, Jr.
Volume XV	Alumina-Condensed Furfuryl Alcohol Resins, by C. W. Boquist, E. R. Nielsen, H. J. O'Neil and R. E. Putcher.
Volume XVI	An Electron Spin Resonance Study of Thermal Reactions of Organic Compounds, by L. S. Singer and I. C. Lewis.
Volume XVII	Radiography of Carbon and Graphite, by T. C. Furnas, Jr. and M. R. Rosumny.
Volume XVIII	High Temperature Tensile Creep of Graphite, by E. J. Seldin.

Volume XIX Thermal Stresses in Anisotropic Hollow Cylinders, by Tu-Lung Weng.

Volume XX The Electric and Magnetic Properties of Pyrolytic Graphite, by G. Wagoner and B. H. Eckstein.

ABSTRACT

Measurements obtained using a carbon arc image furnace indicate that the spectral reflectance and emissivity of carbon and graphite samples in the visible region of the spectrum are strongly dependent on surface finish, but are independent of temperature to at least 3000°K, regardless of surface finish. Discrepancies with other measurements of emissivity are indicated to be caused by errors in the measurement of surface temperature, due to thermal gradients.

Information has been obtained with the carbon arc image furnace indicating that the thermal conductivity of surface material depends strongly on surface finish and is smaller than the conductivity of substrate material.

This technical documentary report has been reviewed and is approved.

W. G. RAMKE
Chief, Ceramics and Graphite Branch
Metals and Ceramics Division
AF Materials Laboratory

TABLE OF CONTENTS

LIST OF ILLUSTRATIONS

LIST OF ILLUSTRATIONS (CONT'D.)

LIST OF TABLES

1. INTRODUCTION

A carbon arc image furnace of new design[1, 2] developed in this Laboratory prior to this study program has been employed to measure high temperature properties of carbon and graphite.

The image furnace, equipped, instrumented, and used as described in this report, provides an almost ideal means for measurement of reflectance and emissivity of opaque materials such as graphite. The measurements carried out in this report have concentrated on a study with typical selected carbon and graphite materials of the effect of temperature, surface finish, and layer plane orientation on the spectral reflectance and emissivity.

Reflected radiation is separated from emitted radiation with samples heated in the image furnace by means of shutters which eclipse the furnace radiation, hopefully so rapidly that the temperature and emitted radiation do not change. Because infinite shutter speed cannot be achieved, a study has been made of the temperature variation immediately after interruption of the furnace radiation incident on the sample. Two related mathematical problems were solved and confirmed by experimental measurements. The experimental measurements have provided a new method for determination of thermal conductivity at high temperatures and have revealed interesting and hitherto unobserved surface effects.

Manuscript released by the authors July 1963 for publication as an ASD Technical Documentary Report.

2. SUMMARY

2.1. Spectral Reflectance and Emissivity of Carbon and Graphite

2.1.1. Conventionally Fabricated Carbon and Graphite Materials

1. The results reported in this report have shown conclusively that the spectral reflectance and emissivity of conventional carbon and graphite materials, either rough or smooth, are essentially independent of temperature from near room temperature to approximately 2300°K. Suggestions have been made to explain the apparently discordant results of other workers in terms of errors in determination of surface temperature due to thermal gradients.

2. There is a slight tendency for the spectral reflectance of the roughened samples to increase with increasing wavelength over the visible portion of the spectrum.

3. Carbon and graphite samples can have a spectral emissivity ranging from as low as 0.70 - 0.75 for polished surfaces to values close to unity for roughened surfaces.

4. Special techniques developed to determine spectral reflectance at the sublimation temperature, 3800°K, show that the spectral emissivity approaches 0.98 and 0.99 respectively for carbon and graphite materials.

2.1.2. Pyrolytic Graphite

Measurements of reflectance on smooth surfaces of pyrolytic graphite samples in the visible region of the spectrum have shown that:

1. The reflectance and emissivity of pyrolytic graphite are within the accuracy of the measurements independent of temperature over the range studied, 500 to 1800°K.

2. The reflectance at 45° angles of incidence and reflectance from smooth surfaces of pyrolytic graphite are in good agreement with approximate calculations (indicating a reflectance in the approximate range 20 to 28 per cent) based on the optical constants of single crystal graphite.

3. The polarization of the reflected light ranges from approximately 20 to 80 per cent, depending upon the orientation of the graphite layer planes relative to the reflecting surface.

2.2. Studies on Heating and Cooling Behavior of Materials in the Arc Image Furnace

These studies of rate of cooling in the arc image furnace have resulted in a useful method for the determination of the thermal conductivity of carbon

and graphite materials at temperatures above 2000°K. The method can be extended above 3000°K and can undoubtedly be applied to other refractory materials. Advantages of this method are as follows:

1. The method requires small quantities of material, approximately one centimeter sample dimensions.

2. The experimental measurement can be accomplished in less than one minute, thereby minimizing high temperature alteration of the material.

3. The method can distinguish between surface material and the underlying bulk material.

The application of this method to a variety of carbon and graphite samples at temperatures near 2500°K has shown that material within approximately one-tenth millimeter of the surface exhibits a much lower thermal conductivity — almost an order of magnitude in the extreme — than the underlying material. The reduction in conductivity of the surface material compared to the substrate material is determined by the manner of the surface preparation and by the nature of the material, being greater for the more graphitic materials.

2.3. Mathematical Solutions to Problems

The following solutions to problems have been applied to the measurements in this report.

1. Appendix I contains an approximate calculation of the reflectance and polarization of light reflected at 45° angle of incidence from single crystal graphite at room temperature.

2. Appendix II contains a solution to the problem of the temperature variation of the surface of a semi-infinite body subjected to a periodic rectangular heat flux.

3. Appendix III contains a solution to the problem of the temperature variation of the surface of a semi-infinite body having initially a constant thermal gradient and subsequently obeying Newton's Law of Cooling.

3. DESCRIPTION OF CARBON ARC IMAGE FURNACE

The characteristics of the carbon arc image furnace used in this work have been reported[1] and application to various measurements has already been described[2]. The work reported herein was done with an arc image furnace using a modified Strong "Super-135" projection lamp equipped with a water-cooled silver contact for the 11 mm diameter "National" "Ultrex"* positive electrodes and a water-cooled copper contact for the 5/16-inch diameter negative electrodes. This electrode combination was operated from a 115-volt direct current motor-generator set with series resistance to give an arc voltage of 75-80 volts at 190-200 amperes.

The arrangement of the image furnace is shown in Figure 1. Both 18-inch diameter reflectors, R_1 and R_2, had silvered second surface glass reflecting surfaces. Two observation holes were positioned at the center and at 45 degrees in reflector R_2.

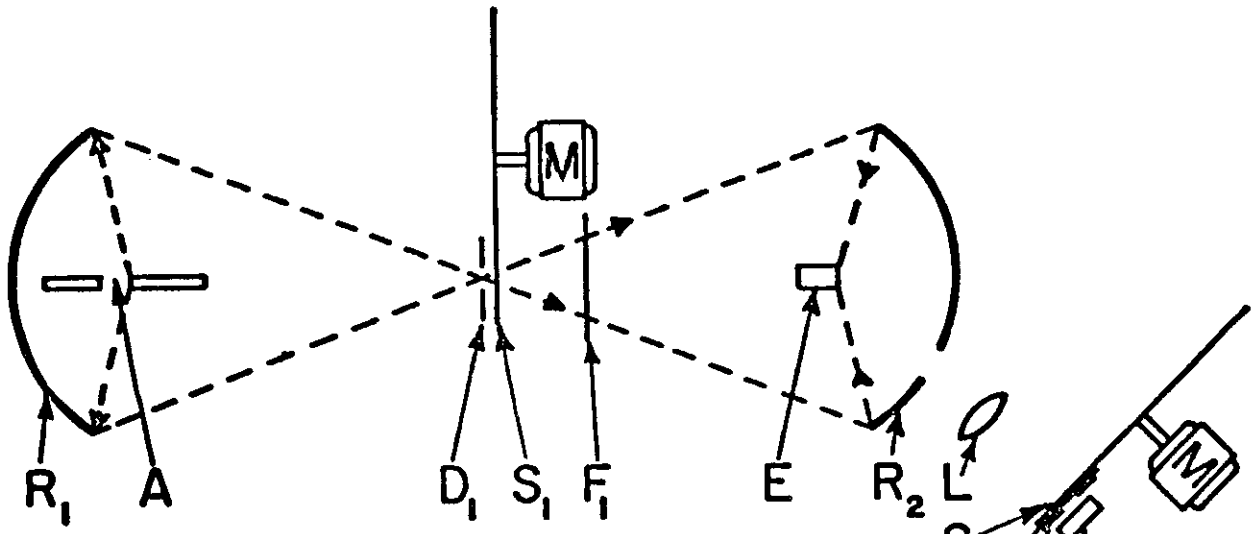

A - Image Furnace Arc, D_1 and D_2 - Diaphragms,
S_1 and S_2 - Synchronous Shutters, L - Lens,
C - Photocell, F_1 and F_2 - Filters, E - Exposed
Sample, M - Motor, R_1 and R_2 - Furnace Reflectors

N-2991

Figure 1. Arrangement of Arc Image Furnace for Reflectance Measurement

The rotating shutters, S_1 and S_2, used to separate the emitted from the reflected sample radiance were 17-inch diameter disks of 1/16-inch thick alloy aluminum and were driven by direct connected 1/8-horsepower synchronous motors. The motor for shutter S_1 at the intermediate focus was mounted so

* "National" and "Ultrex" are registered trademarks of Union Carbide Corporation.

that it could be rotated about its axis and fixed to set the two shutters in any desired phase relationship. The open and closed portions of the two shutter blades were altered for the various test requirements and will be described in the following sections of this report.

Most of the work was performed using a filtered RCA type 929 vacuum photocell as the sensing unit to transfer the optical signal to an electrical impulse which could be displayed on the tube face of a cathode-ray oscilloscope. Other details of the measuring system will be described in the appropriate sections.

4. MEASUREMENT OF SPECTRAL REFLECTANCE AND EMISSIVITY OF CARBON AND GRAPHITE

There are two ways of measuring the spectral emissivity of the surface of an opaque body. One widely used method involves the direct measurement of the spectral radiance of the surface along with a determination of its true temperature. Combination of these data with the black body radiation laws yields the spectral emissivity. Another method measures the spectral reflectance of the surface. From this data the spectral absorptance is calculated and, by application of Kirchhoff's law, is equated to the spectral emissivity. Both of these methods, which we shall designate respectively as "radiation" and "reflection" methods, have limitations which will receive attention in this report.

The principal difficulty with the "radiation" method is the determination of the correct temperature of the radiating surface and strict exclusion of reflected radiation. These conditions become increasingly difficult to maintain at higher temperatures and with materials of lower thermal conductivity. The "reflection" method has the advantage that it does not require determination of the true surface temperature; in fact, the emissivity so determined can be combined with the radiance temperature to provide an accurate determination of the true surface temperature. The most serious problem with the "reflection" method is the separation of reflected from emitted radiation, which assumes ever greater proportions at higher temperatures. This section will deal with the application of a carbon arc image furnace to the "reflection" method for determination of emissivity of opaque materials.

4.1. Measurements Below 3000°K

4.1.1. Procedure

Figure 1 shows a diagram of the carbon arc image furnace and apparatus employed for the measurement of reflectance. The study sample is placed at E and heated by image furnace radiation. The emitted and reflected radiation from the sample at E was measured with an RCA type 929 vacuum photocell connected across a 1000 ohm load resistor to a Tektronix Model 502 cathode-ray oscilloscope. Traces were observed visually or were photographed on a Polaroid camera and measured with a traveling microscope print reader. Lens L and diaphragm D_2 limited the view of the photocell C to an area of 2.3 mm diameter at the sample position. Narrow band interference filters F_2 were used to limit the response of the photocell to a small spectral range near wavelengths 4305, 5010, 5545 and 6080 A. Photographic neutral density filters were also employed at F_2 to attenuate the radiation to keep within the current limitation of the photocell. The direction of observation of E was chosen 45 degrees from the optical axis to facilitate measurement of specular surfaces and to reduce the level of scattered radiation.

The radiation from sample at E at temperatures below 1900°K consisted almost entirely of reflected radiation. Above 1900°K, the emitted component became measurable and was separated from the reflected radiation by 2-blade

rotating shutters S_1 and S_2 driven by 1800 rpm synchronous motors. Shutter S_1 interrupted the furnace radiation and S_2 was placed in front of the photocell and filters to provide a zero signal. Diaphragm D_1 subtended 15 degrees of rotation of shutter S_1. Three different shutter blade widths: 150, 90 and 30 degrees, having transmission values of 1/6, 1/2 and 5/6, respectively, were employed at S_1 to produce corresponding sample temperatures of approximately 1200, 1800 and 2300°K. Shutter S_2 subtended an angle of 7.5 degrees.

When a sample at E having a diffuse surface was observed, the photocell C received radiation from all portions of the reflector R_2. The reflection signal on the oscilloscope was later compared to that from a standard of diffuse reflectance, a layer of at least one mm thickness of freshly deposited magnesium oxide[3-6]. For use at the high radiance levels of the arc image furnace, the magnesium oxide was deposited on a flat, water-cooled copper or silver disk of nominal one inch diameter. The reflectance of the surface of the study sample was determined by using a reflectance value of 0.98[4,5] for the magnesium oxide surface.

When the specimen E had a specular surface, the photocell C received radiation from the one small portion of the reflector R_2 which had the correct angle of incidence. Figure 2 shows schematically this situation for a plane specular surface at E. Location of the active area on the mirror viewed by the surface under investigation was accomplished by positioning an opaque non-reflecting disk of 2.5 inch diameter at various positions over the surface of the mirror until the observed oscilloscope deflection became a minimum. The deflection reduced to zero for a completely specular surface. When less perfect surfaces were measured, the remaining deflection was contributed by the diffuse component of the surface reflectance. Degree of specularity was defined as the per cent reduction in signal produced by the 2.5 inch opaque shield. The reflecting specimen E under study was removed after location of the active mirror area and replaced by a thin polished quartz plate of known index of refraction from which its reflectance at the required angles was calculated. The quartz plate was then positioned so that it had the same disposition relative to reflector R_2 as did the surface under study. This was accomplished by placing a small incandescent bulb in the center of the opaque disk and tilting the quartz plate until the light from the bulb fell upon the photocell. The opaque disk and incandescent bulb were removed and the image furnace radiation was reflected from the mirror by way of the quartz plate into the photocell and the corresponding oscilloscope signal was determined. The reflectance value of the two surfaces of the quartz plate (taking into account the multiple reflections) calibrated the reflected signal for this particular area of the mirror and gave the specular component of the reflectance. The portion of oscilloscope deflection not removed by the opaque disk was treated as the diffuse component and was compared to the magnesium oxide calibration signal. The sum of the two reflectance components gives the total spectral reflectance of the surface under investigation at the 45 degree angle.

The emitted component of the radiance of the study sample was obtained from the oscilloscope signal during the interval when shutter S_1 was closed. The emitted radiation component gave a measure of the radiance (brightness) temperature of the sample. Calibration of the temperature scale of the

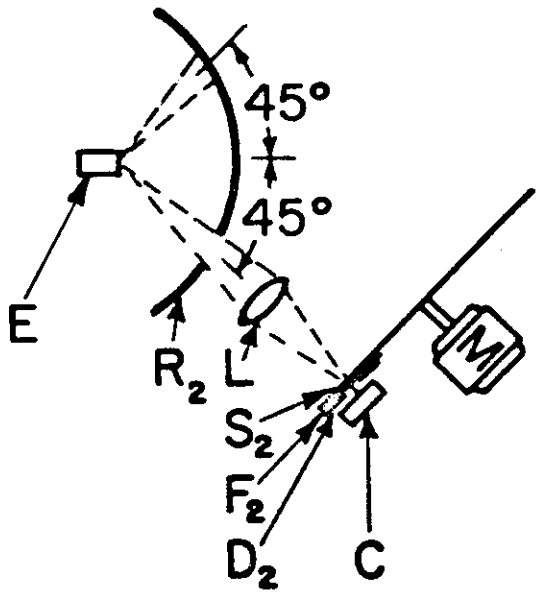

N-3282

Figure 2. Measurement of Reflectance of Specular Surfaces in Arc Image Furnace

photocell-filter-oscilloscope combination was accomplished by observation of a standard source of known spectral radiance temperature. The recently described pyrometric carbon arc [7] which has a radiance temperature of 3800°K was used for calibration purposes in this study and was placed with its crater tip at the sample position of the carbon image furnace. The resultant spectral radiance temperature of the study sample can be converted to true temperature by combination with its measured spectral emissivity.

The total furnace irradiance may be conveniently measured by the use of the water-cooled magnesium oxide disk which is viewed through a small diaphragm by a calibrated thermopile. Previous measurements [8] have shown that 60 to 70 per cent of the arc image furnace radiation falls in the 4000 - 7000 A wavelength range (where MgO has a reflectance near 0.98); only a small fraction falls beyond 10,000 A and none beyond 25,000 A. Measurements of Sanders and Knowles Middleton [6] showed that the reflectance of MgO did not drop below 0.94 out to 24,000 A. Therefore, the mean reflectance of the magnesium oxide disk over the effective range of wavelengths incident upon it was taken as 0.96. The Eppley circular 4-junction copper-constantan thermopile was positioned one meter from the magnesium oxide disk. The output of the thermopile was read with a Leeds and Northrup style 2430 A galvanometer. A diaphragm of 2.6 mm diameter was placed at a distance of 70 cm from the thermopile. These dimensions determined the solid angle and sample area involved, and when combined with the galvanometer deflection and resultant thermopile irradiance, gave the level of furnace irradiance incident on the magnesium oxide disk. The galvanometer-thermopile combination was calibrated in absolute units by means of an NBS carbon filament radiation standard.

Values of furnace irradiance measured in this fashion agreed very closely with those obtained earlier with a calorimeter.

Two types of sample enclosures were employed to protect the carbonaceous samples from oxidation. The simplest of these was an open-end Vycor tube of 12 mm inside diameter through which about one CFM of argon gas was passed. The samples were placed with the exposed face 1/16 inch inside the open end of the tube. This enclosure satisfactorily protected all materials at the 1200°K temperature but was not adequate to preserve highly polished surfaces at the higher temperatures. A closed Pyrex cylinder of 2.5 inch inside diameter with a hemispherical end was used to enclose the samples in an atmosphere of flowing argon for the tests at 1800 and 2300°K.

The materials employed in this study were "National" Special Spectroscopic grades AGKSP graphite and L113SP lampblack-base electrodes. The samples were 3/8 inch diameter and 3/8 inch length and were mounted on 1/8 inch diameter carbon rods and positioned to expose one end to the furnace radiation.

The ends of the graphite and carbon cylindrical samples were both given a final polish on partially used 4/0 Buehler Emery Polishing Paper which rested on a plate glass surface. With a little care, we were able to prepare scratch-free surfaces which measured 85 to 90 per cent specular. The roughened samples were produced by rubbing them across fresh 80-grit garnet paper with care being taken to avoid polishing action by particles of graphite which lodged in the grains of the abrasive paper. In this respect, the AGKSP graphite samples were more critical than the L113SP lampblack ones.

4.1.2. Experimental Results

Table 1 gives the spectral reflectance and emissivity as measured at ~ 1200°K in the open end tube with the 150 degree wide shutter blade for the two surface finishes of both kinds of carbon material. The reflectance data are also plotted in Figure 3. The polished surface for both grades of carbon shows no significant wavelength dependence for the reflectance over the visible portion of the spectrum; a horizontal straight line falls within the range of measured values. The range of values of ± 10 per cent although partly due to measurement errors, may be attributed more to the lack of reproducibility of the polished surfaces.

The roughened surfaces show a very slight increase in spectral reflectance in going from the blue to the red end of the spectrum, an increase which is hardly greater than the approximate 10 per cent spread of values at each wavelength. However, this trend toward increasing reflectance at longer wavelengths has been observed by numerous workers [9, 10].

The absolute reflectance values are in reasonable agreement with those previously reported [9]. The lampblack-base material produces slightly lower spectral reflectance than the graphite specimens for both surface finishes. The reflectance observed at 45° angle of incidence for the polished surfaces, particularly for the AGKSP graphite material, is very close to the values

Table 1. Spectral Reflectance and Emissivity of Polished and Roughened Surfaces of Grades AGKSP Graphite and L113SP Carbon Measured in the Arc Image Furnace

Material	Temp. °K	4305 A		5010 A		5545 A		6080 A	
		r	ε	r	ε	r	ε	r	ε
AGKSP POLISHED	1180	0.273	0.727	0.284	0.716	0.297	0.703	0.292	0.708
AGKSP ROUGHENED	1220	0.050	0.950	0.054	0.946	0.053	0.947	0.059	0.941
L113SP POLISHED	1230	0.251	0.749	0.243	0.757	0.251	0.749	0.243	0.757
L113SP ROUGHENED	1250	0.030	0.970	0.033	0.967	0.031	0.969	0.035	0.965

°K, Surface temperature; r, Reflectance; ε, Emissivity

Data measured at 45° Angle in Open-End Tube with Argon Flow.

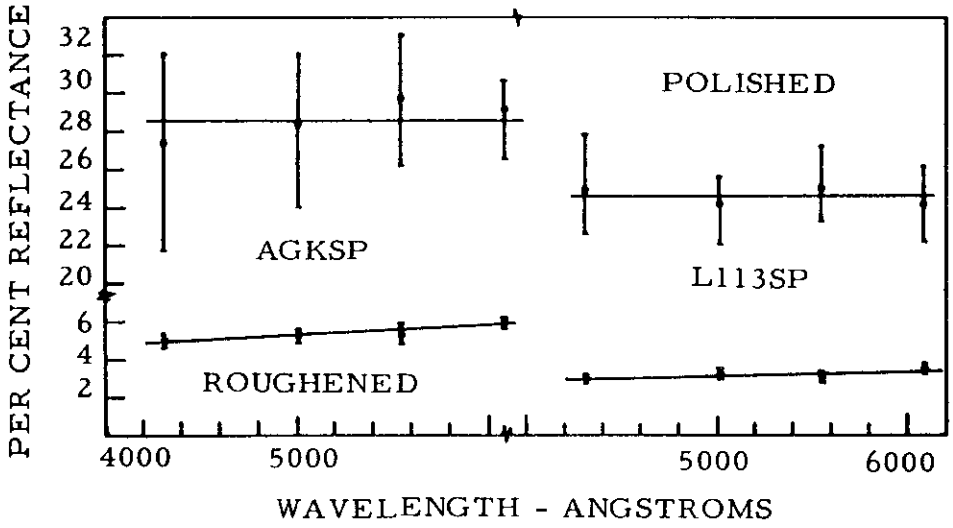

N-3285

Figure 3. Spectral Reflectance of Grades AGKSP Graphite and L113SP Carbon at 45° Angle and 1200°K Temperature

measured by McCartney and Ergun [11] perpendicular to the basal planes of single crystal graphite, 27.7 - 28.0 per cent at 5500 A. The reflectance for the roughened surfaces approaches the low values which have been observed for oxidized or sublimating graphite [2, 12].

Additional data for spectral reflectance at temperatures as high as 2200 to 2400°K showed no dependence on temperature. This fact is most convincingly shown in Figure 4 which gives an oscilloscope trace obtained over a period of 50 seconds, with the shutter running for a roughened AGKSP sample while heating from room temperature to final value. The top trace (emitted plus reflected radiance) in each oscillogram gives the locus of the signals with shutter S_1 open while the intermediate trace, when resolved, refers to shutter S_1 closed (emitted radiance) and the bottom trace is a zero signal. Figure 4 shows no significant change in the reflected component from the start at room temperature to the final temperature. The final temperature was ~ 1200°K in the right oscillogram (S_1 = 150°) and ~ 2200°K in the left one (S_1 = 30°). Emitted light was evident only at the highest temperature, which was reached after ~ 15 to 20 seconds. These and many other traces for both polished and roughened surfaces, using either grade of carbon, show clearly that the reflectance and emissivity are unchanged up to temperatures of 2200 - 2400°K.

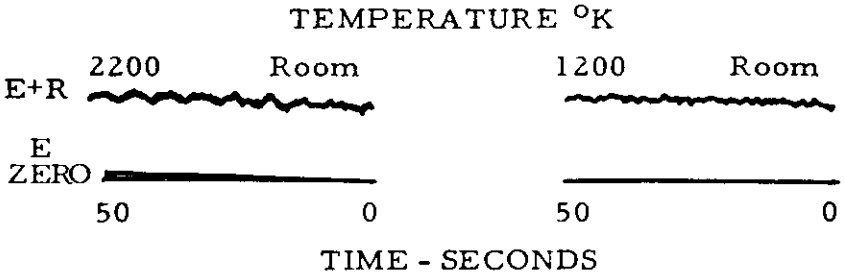

N-3283

Figure 4. Radiance Signal vs. Heating Time for Roughened Grade AGKSP Graphite

4.1.3. Discussion of Results

Results of previous workers on the emissivity of carbon and graphite have recently been summarized in excellent fashion by Plunkett and Kingery [9]. Subsequent papers by Grenis and Levitt [13] should also be mentioned. The earlier results have shown wide differences. Except for highly polished surfaces, the spectral emissivity of carbon and graphite (generally determined near 6500 A) has shown a marked tendency to decrease with increasing temperature. The trends have been such that the corresponding spectral reflectance would have shown increases of as much as 50 per cent in the temperature range from 1000 to 2000°C, a variation which would have been easily observable in the present study. The fact that no significant temperature dependence has been observed with the arc image furnace calls for a search for another explanation which will be discussed later.

The marked exceptions to the decreasing spectral emissivity with increasing temperature are the results for highly polished materials, for which Thorn and Simpson [14], Plunkett and Kingery [9], and Grenis and Levitt [13] have obtained spectral emissivity values which are almost independent of temperature in the 1000 - 3000°C range.

The careful studies of Warmuth [15] with a "reflection" method also deserve comment. Warmuth measured the spectral reflectance in the visible region of the spectrum for the rough surface of a nongraphitic carbon material over the range from room temperature to 1740°K. The spectral reflectance was found to be very close to 3 per cent and showed no significant variation with temperature; both of these results are in close agreement with the results of the present report.

Plunkett and Kingery [9] also reported a careful series of tests on one graphite material given various degrees of surface roughness. This series showed that the rougher the surface, the greater the spectral emissivity at low temperatures and the greater its decrease with increasing temperatures.

Grenis and Levitt[13] reported similar experience from measurements on rough machined and polished surfaces of the same base material.

The results on the temperature dependence of spectral emissivity by other workers showing decreasing emissivity with increasing temperature have all been obtained using a "radiation" method. The "radiation" methods for determining spectral emissivity depend, through application of Wien's or, more properly, Planck's Law, upon a direct measurement of the radiance temperature of the surface under study and upon a determination of the true temperature of the surface. Determination of the true surface temperature always entails another measurement of temperature at some location more or less distant from the area of the radiating surface under study and requires somewhat uncertain corrections to compensate for the spatial separation of the two locations. A spurious decrease in the calculated spectral emissivity can result if the value taken for the true surface temperature is too high. Such a high value can result, for example, from thermal gradients through the sample set up by the radiated flux. The magnitude of such an error depends, in part, upon the thermal conductivity of the material near the surface and becomes more marked at higher temperatures, where the radiated flux and associated thermal gradient are larger.

Careful consideration suggests that the discrepancy between the temperature variation of spectral emissivity of roughened materials as determined by "reflectance" and "radiation" methods arises from the effect of the surface layers on the thermal gradients discussed in the preceding paragraph. The following discussion considers these factors in more detail.

Table 2 presents a tabulation of factors pertinent to this problem. Columns 1 and 2 show the magnitude of thermally radiated flux for various temperatures. Column 3 lists the change in black body temperature for a 10 per cent change in the spectral radiance at the common pyrometric wavelength. Such errors in temperature of the surface would result in errors in spectral emissivity with the "radiation" method in the range of the observed discrepancies from the values obtained by the "reflection" method. For example, assigning a surface temperature 18.2°K too high at 2000°K would result in a spectral emissivity 10 per cent too low, would lower a true emissivity of 90 per cent to an incorrect calculated value of 81 per cent, and would indicate an incorrect reflectance of 19 per cent rather than the correct value of 10 per cent. Based on typical thermal conductivity for graphite, a thermal gradient of 180°K/cm associated with the radiated flux would result in a temperature difference of the indicated magnitude with an effective thermal conduction path of only one millimeter. With some of the experimental arrangements that have been used, it is difficult, if not impossible, to rule out such errors. Table 2 makes it clear that errors due to thermal gradients increase extremely rapidly with increasing temperature. Even more serious are indications presented later in this report that the attenuation of the roughened surface layers increases the surface resistivity several-fold. For example, Section 5.1.8. indicates that material within approximately one-tenth millimeter of the surface may have thermal conductivity as low as one-fifth the values shown in Table 2 and would develop the indicated temperature error over an effective path length of only a few tenths millimeter.

Table 2. Radiant Flux and Associated Thermal Gradient

Temp. °K	Black Body Radiation watts/ cm^2	Temp. Change for 10 Per Cent Change in Spectral Radiance* °K	Thermal Conductivity** watts/cm^2 /°K	Temp. Gradient*** °K/cm	Effective Path Length for Temperature Change of Column 3 cm
1000	5.7	4.5	1.0	5.7	0.8
1500	29.0	10.4	0.8	36.3	0.3
2000	90	18.2	0.5	180	0.1
2500	220	29	0.4	550	0.05
3000	450	42	0.3	1500	0.03

* At 0.66 micron wavelength
** Typical grade of graphite
*** Temperature gradient due to radiated flux

4.2. Measurements at Sublimation Temperature

Studies were made using the carbon arc image furnace to measure the spectral reflectance and emissivity of carbon and graphite at the sublimation temperature. Special problems were encountered and new procedures were developed as described below.

4.2.1. Procedure

The arrangement of the image furnace and associated apparatus was essentially the same as shown in Figure 1. The graphite or carbon surface to be studied was the crater face of the positive electrode of an electric arc, the so-called "pyrometric arc" recently described by the authors [7], used to maintain the crater of the positive electrode at a consistent temperature of 3800°K. The crater face was placed at the sample heating position E in the carbon arc image furnace which provided radiation for determination of the reflectance.

The diaphragm D_2 was reduced in size to limit the view of the photocell C to an area of 1.15 mm diameter at E. The load resistor across the photocell was increased to 4700 ohms to provide adequate signal.

The measurement of reflectance in these tests with the arc image furnace depends on the separation of reflected from emitted radiation by a rapidly rotating shutter S_1 which alternately interrupts and transmits the radiation from the image furnace for 5/360 and 1/360 second intervals (1800 rpm shutter, 2-30° openings). If the emitted radiation remains unchanged during the short interval (less than 1 millisecond) required to close or open the shutter, then

one can measure the reflected component of the radiance of the sample by measurement of the radiance immediately before and after closing or opening the shutter. However, any change in the temperature and emitted radiance of the surface which is rapid enough to occur during the time required for the edge of the shutter to traverse the beam would erroneously be classed as "reflected" radiation. The following experiments have shown the existence of such rapid heating effects and the means of correcting for them to obtain the true reflectance.

The image furnace radiation was passed through a "stock thickness" Corning H.R. 2-58 red glass filter placed at F_1 which removed all visible radiation within the responsive wavelength range of the photocell but transmitted longer wavelength red and infrared radiation sufficient to produce an irradiance on the crater face amounting to a little more than half of the unfiltered value. Separate tests performed by reflecting this filtered radiation from magnesium oxide deposited on the surface of a water-cooled copper disk confirmed that the photocell indeed was not affected. Nevertheless, when this radiation was allowed to pass through the 30° openings of shutter S_1 and fall on the hot arc electrode surface at E, it produced a measurable increase in spectral radiance, necessarily due to an increase in temperature of the crater surface. A sample oscillograph trace for the heating of a graphite electrode is shown in Figure 5. The profile of the oscillograph traces generally showed the increases in temperatures to be essentially completed during the less than one millisecond time required to open or close the shutter and showed little evidence of any subsequent heating or cooling during the completely open or closed portions of the shutter cycle.

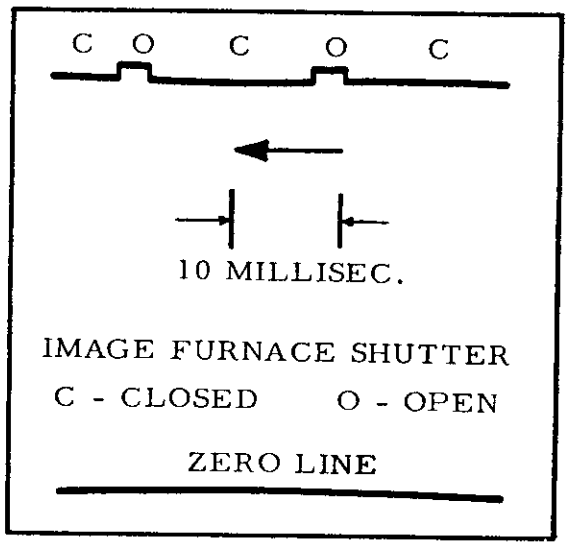

N-2992

Figure 5. Oscillograph Trace of Crater Radiance at 4305 A for Grade AGKSP Graphite Electrode Irradiated by Arc Image Furnace Through Corning H.R. 2-58 Red Glass Filter

The increase in spectral radiance was measured relative to that of the background of emitted radiation from the crater. The results are plotted in Figure 6 for three different wavelengths and for three different types of 1/4-inch diameter "National" spectroscopic electrode materials with the properties shown in Table 3. The solid lines show the increases in spectral radiance expected for 18°K and 48°K temperature increases at 3800°K, the known radiance temperature of the crater. Within the accuracy of the measurements, the data fit black body radiance increases of 18°K for the Grades AGKSP and SPK graphite electrodes and 48°K for the Grade L113SP carbon electrodes. The greater temperature increase for the carbon electrode is no doubt related to its lower conductivity. The close fit of the data to the black body curves in Figure 6 indicates that the increase in radiance results from changes in temperature of the crater caused by the absorbed radiation.

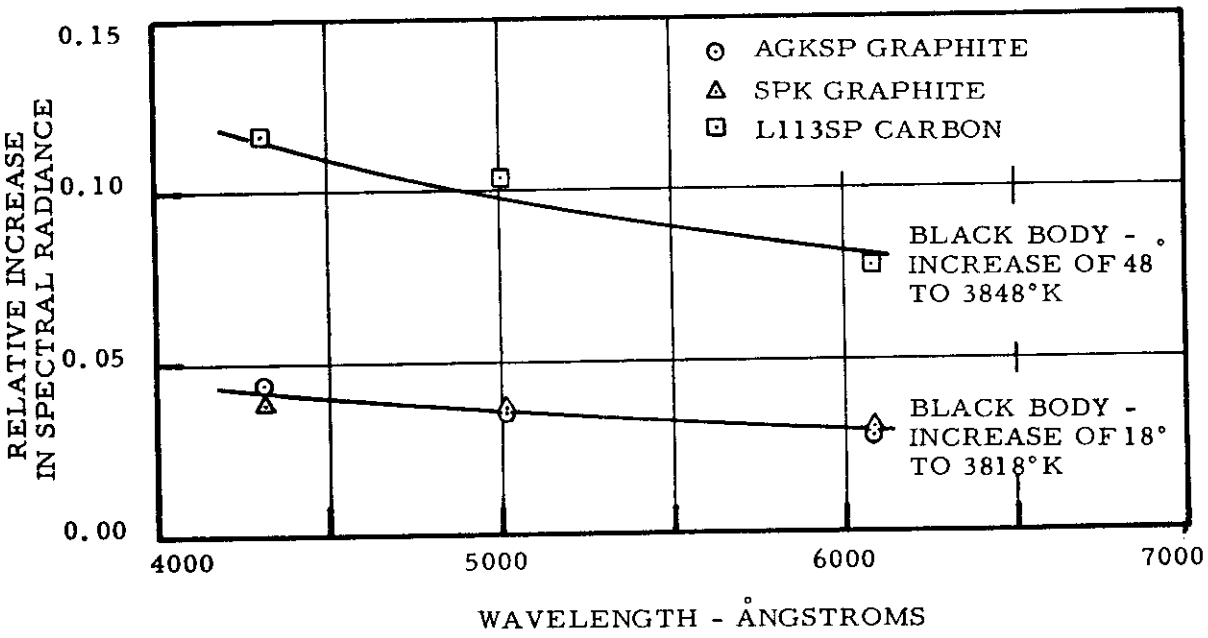

N-2988

Figure 6. Increase in Spectral Radiance of Pyrometric Arc Crater Produced by Carbon Arc Image Furnace Radiation Filtered Through Corning H.R. 2-58 Red Filter, 4.7 Watts per sq. mm Instantaneous Flux through Shutter with 0.167 Transmission

Table 3. Typical Physical Properties of "National" Spectroscopic Electrodes Used in Reflectance Measurements

Grade	Type	Bulk Density, g/cc	Resistivity ohm - inch	Maximum Ash - pph
AGKSP	Graphite	1.61	0.00025	10
SPK	Graphite	1.90	0.00045	10
L113SP	Graphite	1.45	0.0025	10

The radiant flux transmitted by the red filter was further attenuated by passage through one and two Nichrome wire screens. The solid line in Figure 7 shows that the magnitude of the increase of spectral radiance at 5010 A, measuring the heating of the crater surface, was nearly linearly dependent on the total irradiance incident on the crater. Total irradiance of the image furnace radiation was measured by viewing a magnesium oxide coated, water-cooled disk through a small diaphragm with a calibrated thermopile. From the reflectance of the magnesium oxide, the dimensions of the diaphragm and the calibration of the thermopile, the level of irradiance of the magnesium oxide disk may be determined (see Section 4.1.1.).

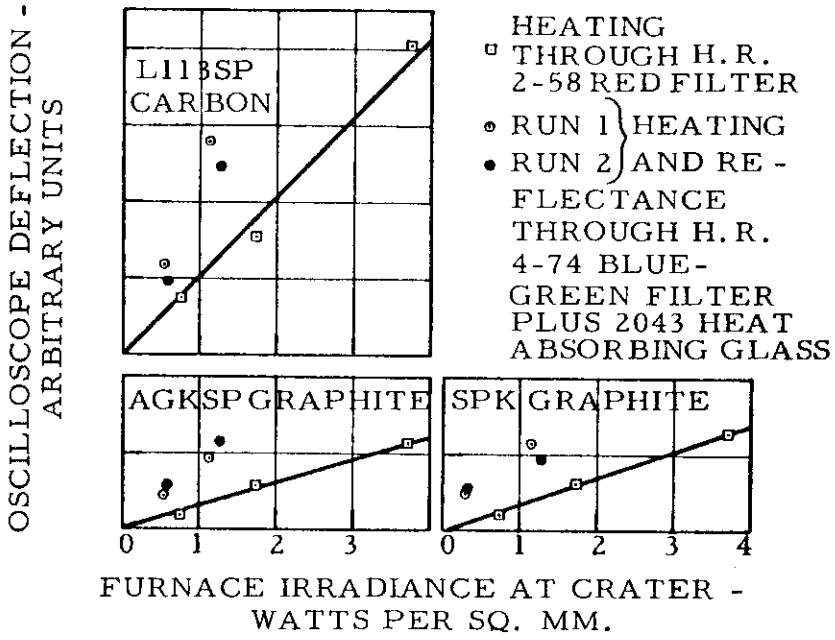

N-2990

Figure 7. Reflectance and Heating of Carbon and Graphite Craters at 5010 A Wavelength

The following procedure was adopted to measure the spectral reflectance of the crater, corrected for the rapid heating described above. The radiation from the image furnace was filtered at F_1 to reduce greatly the quantity outside the wavelength sensitive range of the photocell-filter combination. It was passed through a Pittsburgh Plate Glass Company 2043 phosphate infrared absorbing filter of 2 mm thickness and through a "stock thickness" of either a Corning H.R. 3-66 orange glass filter for measurements at 6080 A or a Corning H.R. 4-74 blue-green filter for measurements at 4305 A and 5010 A. The oscilloscope deflection included the effects of both reflectance from and

heating of the sample but measurement of the total radiant flux incident on the sample permitted a correction for the heating effect of the furnace radiation. Figure 7 shows the oscilloscope deflections plotted at the correct flux values. The excess deflection above the heating curve represents the component due to reflection. Two levels of radiation were used, the lower of which represents interposition of a single Nichrome wire screen, and the results of two independent runs are shown in Figure 7. Calibration of the reflectance measurements was accomplished using a water-cooled, magnesium-oxide smoked surface as a reflectance standard (see Section 4.1.1.).

4.2.2. Experimental Results

The results of Figure 7 and similar measurements at the other wavelengths are listed in Table 4 and plotted in Figure 8.

Table 4. Spectral Reflectance* and Emissivity of Carbon and Graphite at the Sublimation Temperature

Grade	4305 A		5010 A		6080 A	
	Reflectance	Emissivity	Reflectance	Emissivity	Reflectance	Emissivity
AGKSP	0.013	0.987	0.012	0.988	0.014	0.986
SPK	0.014	0.986	0.011	0.989	0.012	0.988
L113SP	0.024	0.976	0.020	0.980	0.024	0.976

* Measured at 45° from normal to surface

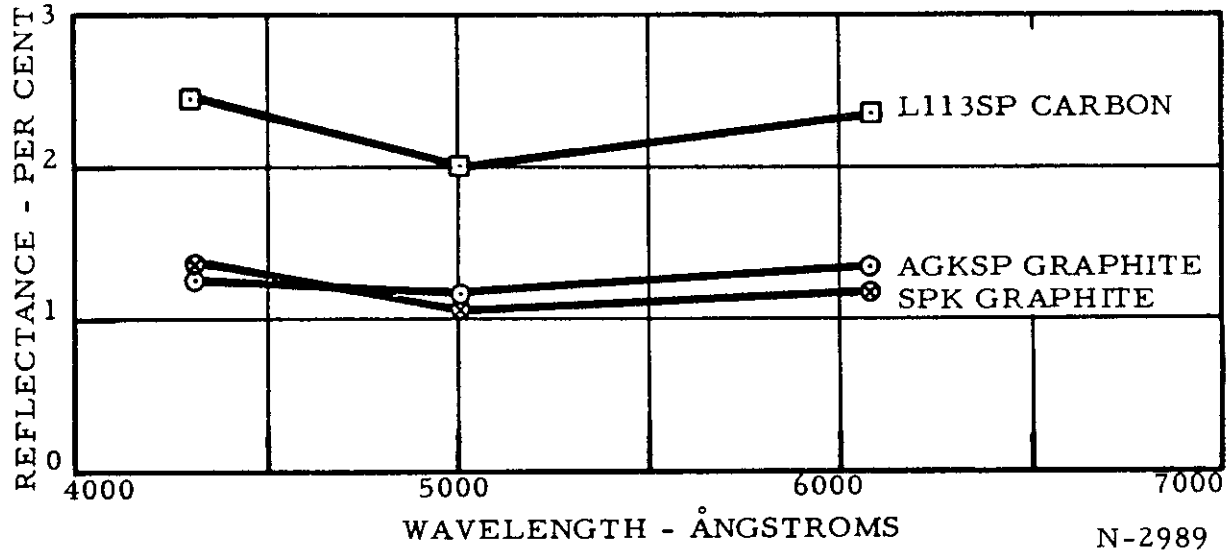

Figure 8. Spectral Reflectance of Spectroscopic Carbon and Graphite Electrodes at 45° Angle and a Surface Temperature of 3800°K

Figure 8 shows that the reflectance at the 5010 A wavelength (green) is approximately 10 to 20 per cent lower than that at the 4305 A (blue) or 6080 A (red) wavelengths. This phenomenon is believed to be real since it has been observed repeatedly in these tests and since some similar indications were obtained several years ago[2].

The Grades AGKSP and SPK graphite electrodes both show a reflectance slightly in excess of 1 per cent. The reflectance of the Grade L113SP carbon electrode is 2 per cent or a little more. The graphite materials are more crystalline and more highly oriented than the carbon. The orientation present in the graphite electrodes exposes predominantly low reflectance edges of the graphite crystals compared with a more random orientation in the carbon electrode.

From the reproducibility of the reflectance data, it is believed that they are generally precise to $\pm$ 0.002 and never in excess of $\pm$ 0.004. The emissivity values in Table 4, obtained by subtraction of the reflectance from unity, have the same precision as the reflectance. The errors result from the fact that the reflection and heating signals were no more than 5 per cent of the emitted light signal, the noise of which constituted a limiting factor.

The measurements presented here for the reflectance and emissivity of carbon and graphite at the sublimation temperature have greater accuracy than those previously presented[2], chiefly because the rapid heating and cooling of the crater by the image furnace radiation which had previously been masked in the reflectance signal have now been measured and taken into account. The improvements were made possible through substitution of the cathode ray oscilloscope and vacuum photocell for the earlier recording microammeter and barrier layer photovoltaic cell.

The graphite craters with their emissivity near 0.99 are a close approximation to a black body radiator in the visible region. This agreement confirms radiation measurements recently reported on these same sources[7]. This high emissivity is due in large measure to the roughened surface produced by the sublimation. Measurement of the reflectances of these craters at lower temperatures show little change from the values measured at the sublimation temperature.

The only similar measurements of the reflectance and emissivity of graphite at the arc temperature are those reported by Euler in Germany[16-19]. However, Euler's values for the reflectance have been shown[2] to be approximately ten times too high.

The methods described in this paper possess wider utility than the examples presented and promise to clarify effects of surface structure on emissivity. These procedures may be extended to other methods of heating. For example, heating can be accomplished resistively or inductively and the image furnace, as here, may be used to measure reflectance.

The extremely rapid response of the crater surface to incident radiation bespeaks an exceptionally low thermal conductivity or thermal inertia of the surface material. The same behavior was also noted by Euler[18].

4.3. Reflectance and Emissivity of Pyrolytic Graphite

Some work was carried out early in the study period to determine the reflectance (and emissivity) of pyrolytic graphite at elevated temperatures. It is well known[20] that pyrolytic graphite suitably prepared has physical properties which approach closely many of those of single crystal graphite. Because pyrolytic graphite can be prepared in more massive sizes than single crystal graphite, particularly as regards thickness, the pyrolytic variety offers the possibility of studying some properties which are otherwise difficult or impossible to determine. Such is the case with the reflectance and emissivity of graphite for surfaces cut across the layer planes.

The image furnace arrangement for this work was essentially the same as shown in Figure 1 and the method of measurement was similar to that previously described[2]. The test samples were placed in a Vycor container protected from oxidation by flowing argon gas. Cell C was a Weston "Photronic" cell fitted with a "Viscor" filter, which gives a combined spectral response approximating that of the human eye. The output of the cell was connected to a General Electric recording microammeter to determine both the emitted and reflected light from the sample. Polarization values were obtained by placing a Polaroid filter between S_2 and L in Figure 1 and rotating it to get the reflectance values for light polarized parallel and perpendicular to the plane of incidence. Forty-five degree angles of incidence and reflectance were used in all cases.

The optical properties of single crystal graphite at room temperature are known from the work of McCartney and Ergun[21]. The index of refraction varies from 2.15 with the electric vector of the light wave in the layer planes to 2.00 with the electric vector across the layer planes. The absorption index varies from 1.42 with electric vector parallel to the layer planes to 0.02 with the electric vector perpendicular. The reflection formulas have not been worked out for anisotropic highly absorbing media other than at perpendicular incidence; however, approximate extensions of the isotropic metallic reflection formulas have been made by us as shown in Appendix I to obtain the expected reflectance and polarization of the light reflected from the graphite crystal at 45° angles of incidence and reflection with layer planes parallel and perpendicular to the surface as shown in Table 5.

Table 5. Calculated Reflectance and Polarization of Light of Wavelength 5500 A Reflected at 45° Angle from Graphite Single Crystal

Case No.	Orientation of Layer Planes	Reflectance Per Cent	Polarization Per Cent
1.	Parallel to Surface	28.6* to 22.1	40.5* to 82
2.	Perpendicular to Surface and Parallel to Plane of Incidence	20.2	15.8
3.	Perpendicular to Surface and Perpendicular to Plane of Incidence	28.1 to 21.8*	43 to 85*

* Correct values are believed close to starred (*) numbers as discussed in Appendix I

Pyrolytic graphite prepared on prior Contract No. AF 33(616)-5563[2], closely approximates the crystal structure and other properties of single crystal graphite and offers macroscopic pieces large enough for study.

Rectangular pieces of this pyrolytic graphite, a few millimeters in size, having a density more than 2.2 grams per cc, were cut with surfaces parallel and perpendicular to the layer planes. These pieces were placed in a graphite holder for mounting in the furnace. The samples were metallographically polished and the polishing debris was removed either by ultrasonic cleaning or, preferably, by cathodic etching in a glow discharge. In this manner, it was possible to remove polishing debris without serious destruction of the optical surface finish (preservation of 60-80 per cent specularity as defined in Section 4.1.1.). Measurements of reflectance and polarization showed no variation over the temperature range 500° - 1800°K; average values are shown in Table 6 along with the corresponding expected values for single crystal graphite from Table 5. Agreement with expected values of reflectance and polarization are, in general, good. The close agreement of the experimental to the starred (*) calculated values confirms the arguments relative to their choice (see Appendix I).

Table 6 shows that surfaces polished but not cleaned approximate the polarization of graphite with layer planes parallel to the surface either with the polycrystalline grade AGKSP manufactured graphite or with pyrolytic graphite. Other tests, not reported here, have shown that the reflectance likewise approaches Case 1. This observation confirms that polishing is primarily a process of mechanical alignment of layer planes of graphite crystallites.

Figure 9 shows the results of a careful evaluation of the effect of temperature on emissivity (reflectance) and polarization with a series of samples having about 60 per cent specularity. Due to poorer surface smoothness, these samples do not show as good agreement with the predictions as Table 6, but they show the lack of any significant variation with temperature. Measurements could not be carried above 1500-1800°K because of rapid surface deterioration with layer planes perpendicular to the surface, even though an argon atmosphere was introduced to retard deterioration.

Plunkett[9] reported measurements of spectral emissivity on four samples of pyrolytic graphite with different surface finish over approximately the same temperature range as Figure 9. Plunkett's samples (all having the orientation of our Case 1), like ours, showed no change of emissivity with temperature, Plunkett's machine-ground and polished samples all showed lower emissivity than his as-deposited material which approached our Case 1 values.

It is interesting to note that edge-cut samples of pyrolytic graphite (cases 2 and 3), suitably polished, can alter the polarization of the reflected visible light from approximately 20 to 80 per cent depending on the alignment of the layer planes relative to the plane of incidence. Application of a thin sheet of pyrolytic graphite as a transmission polarizer for infrared radiation has been described by Rupprecht, Ginsberg and Leslie[22].

Table 6. Reflectance and Polarization of Light Reflected at 45° Angle from Polished and Cleaned Pyrolytic Graphite

Sample	Orientation	Reflectance Per Cent Meas.	Reflectance Per Cent Calc.	Polarization - Per Cent Diffuse Meas.	Polarization - Per Cent Specular Meas.	Polarization - Per Cent Specular Calc.	Polarization - Per Cent Total Meas.
	Layer Planes Parallel to Surface - Case 1						
1	Polished and cleaned	26.3			47.2		
2	Polished and cleaned	25.0			39.5		
3	Polished and cleaned	24.8			40.8		
		24.8	(28.6*-22.1)		42.5	(40.5*-82)	
	Layer Planes Perpendicular to Surface and Parallel to Plane of Incidence - Case 2						
4	Polished and cleaned	16.5		20.1	22.8		21.0
5	Polished and cleaned	17.6		19.8	24.6		23.4
6	Polished and cleaned	20.2		13.8	23.1		15.6
		18.1	(20.2)	17.9	23.5	(15.8)	20.0
7	Polished and not cleaned				38.0		
8	Polished and not cleaned				44.1		
					41.0		
	Layer Planes Perpendicular to Surface and to Plane of Incidence - Case 3						
4	Polished and cleaned	20.7		66.6	82.9		76.0
5	Polished and cleaned	18.6		70.6	74.0		74.0
6	Polished and cleaned	21.3		73.4	81.0		78.4
		20.2	(28.1-21.8*)	70.2	79.3	(43-85*)	76.1
7	Polished and not cleaned				53.7		
8	Polished and not cleaned				46.0		
					49.9		
	Grade AGKSP Graphite						
9	Polished and not cleaned				36.2		
10	Polished and not cleaned				38.2		
					37.2		

* Calculated values taken from Appendix I with starred numbers (*) believed close to correct values.

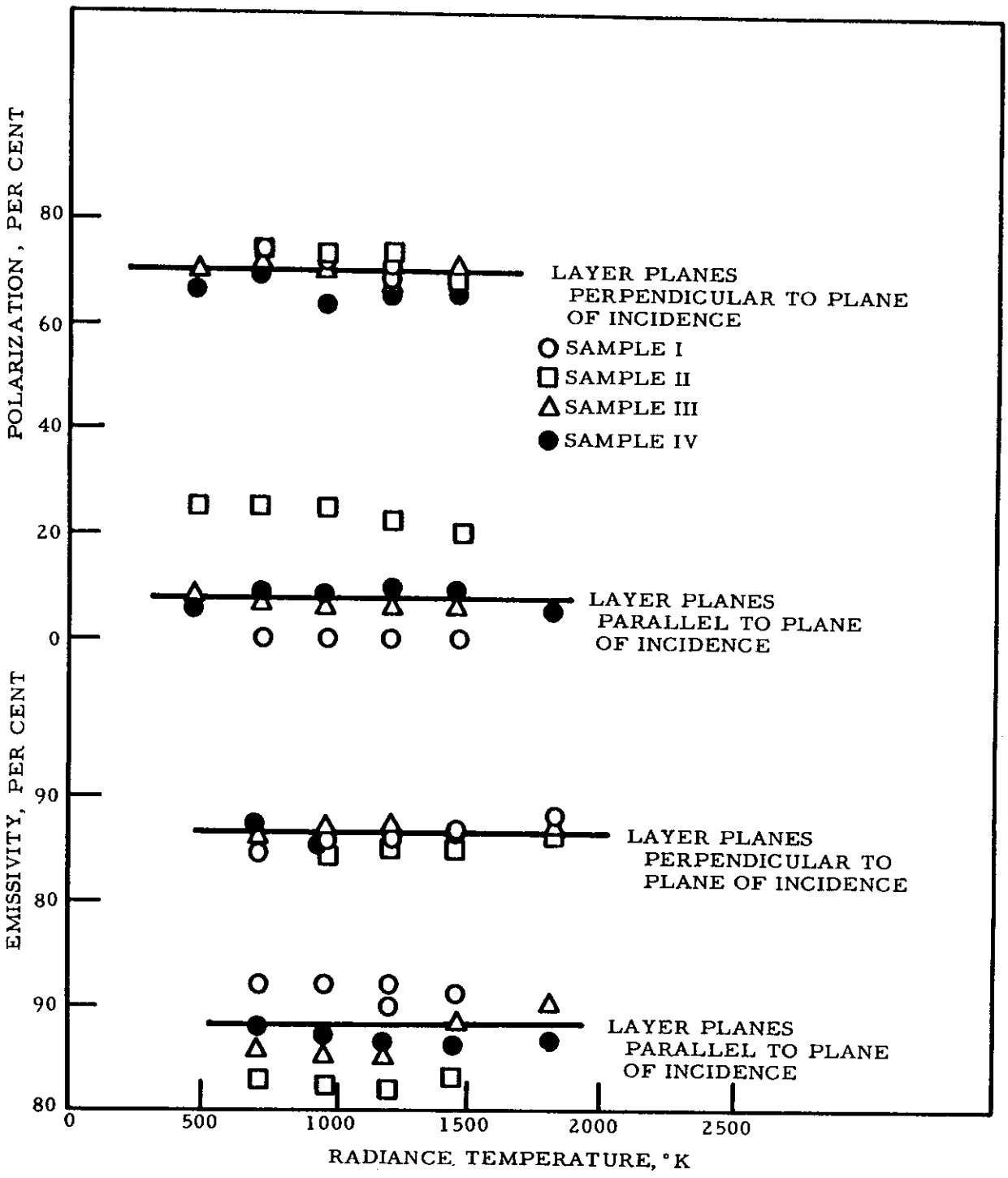

N-816

Figure 9. Emissivity and Polarization vs. Temperature for Polished and Cathodically Etched Surface of the Ends of Layer Planes of Pyrolytic Graphite Measured at 45° Angle

5. STUDIES ON HEATING AND COOLING OF MATERIALS HEATED IN THE ARC IMAGE FURNACE

5.1. Measurements of Rate of Cooling

5.1.1. Introduction

Section 4 of this report has described the measurement of emissivity of carbon and graphite at elevated temperatures by means of the carbon arc image furnace. This section will report the application of the furnace to the study of other material properties such as thermal conductivity.

When a material body is heated in the arc image furnace, a balance is achieved between the absorbed radiation and the various heat losses: emitted radiation, conduction and convection. After the incident furnace radiation is interrupted, the absence of absorbed radiation results in a redistribution among the various loss components and in a change in temperature of the body which is a function of both time and position in the body. The temperature of the surface of the body through which the furnace radiation is absorbed is of most interest because this surface is readily observable.

Two related problems, periodic and nonperiodic interruption of radiation, are treated in Appendixes II and III,respectively. The application of both of these solutions to the study of material properties will be discussed.

5.1.2. Periodic Interruption of Furnace Radiation

Appendix II treats the variation of the surface temperature of a semi-infinite body subjected to periodic rectangular pulses of heat flux at the surface. Since a finite body can be considered to behave as a semi-infinite one under certain conditions of symmetry and uniformity of surface temperature and during sufficiently brief intervals. The results of Appendix II are applicable to the usage of rapidly rotating shutters to interrupt the furnace radiation.

As shown in Equation (6) of Appendix II,

$$\Delta T_C \left[(b-a)\tau\right]^{-1/2} = 2\, H_o (\pi K c \rho)^{-1/2} v_C$$

where ΔT_C measures the change of surface temperature over the time $(b-a)\tau$ measured from the beginning of the cooling phase; a and b measure respectively the heating and cooling fractions of a complete cycle of time τ; H_o represents the instantaneous flux absorbed at the surface; and K, c and ρ refer to the thermal conductivity, specific heat and density of the material. Since v_C is negative, as shown in Table 11 in Appendix II, ΔT_C measures the decrease in temperature during a cooling phase.

As shown in Table 11 and Figure 16 of Appendix II, v_C decreases from an initial value of unity at the start of a cooling interval. However, v_C can be kept near unity throughout a cooling interval by choosing a sufficiently large value of

the heating fraction, a. If all the quantities on the right-hand side of Equation (6) of Appendix II are constant during the cooling interval, then their product can be determined from the slope of the plot of ΔT_C vs. the square root of the time of cooling. Variation of the heat loss H_o with time will be chiefly dependent on the variation of the radiation component, which amounts to four times the fractional change in absolute temperature and can be limited by reducing the total temperature variation by increasing either the interruption frequency or the heating fraction, a. Note that K, c, and ρ are likewise essentially constant for small variations in temperature.

5.1.3. Nonperiodic Interruption of Furnace Radiation

Appendix III treats the variation of the surface temperature of a semi-infinite body having a constant thermal gradient at time zero. This problem is representative of the cooling after interruption of the furnace radiation for a body already heated to equilibrium temperature. Equation (7) of Appendix III shows that the cooling of the surface of the body after a short time t may be expressed by:

$$\Delta T(0,t) \cong 2 (R_o + F_o) \left(\frac{t}{\pi K c \rho} \right)^{1/2},$$

where R_o measures the heat losses from the surface and F_o the conducted flux into the body at time zero, and K, c, and ρ have the same significance as described above.

From the above equation,

$$\Delta T(0,t)\, t^{-1/2} \cong 2 (R_o + F_o) \left(\frac{1}{\pi K c \rho} \right)^{1/2}$$

If the right-hand side of the equation is constant, its value can be determined from the slope of the straight line plot of the decrease in surface temperature vs. the square root of the time of cooling.

The discussion in Appendix III treats the limitations to the first order approximation used in the derivation of Equation (7). The principal limitation arises due to departures from Newton's law of cooling assumed in the solution. However, the length of cooling time permissible for the linear approximation is considerably longer than in the case of the periodic interruption treated in Appendix II.

5.1.4. Effect of Finite Time of Shutter Closure

The effect of finite time required to interrupt the furnace radiation by means of a mechanical shutter has been investigated mathematically. Analysis shows that excellent compensation for this error is achieved by measuring the time of cooling from the middle of the shutter closing interval. The calculations indicate that the value of $\Delta T\, t^{-1/2}$ so determined at the end of the shutter closure has reached a value approximately 95 per cent of the ideal abruptly interrupted value, and one-half shutter closure interval later, the accuracy is 99 per cent.

5.1.5. Experimental Studies of Cooling

Studies have been made on the cooling of bodies in the arc image furnace after interruption of the furnace radiation using both periodic and nonperiodic interruption. The image furnace was essentially as shown in Figure 1.

The rotating shutter at S_1 in Figure 1 consisted of two blades, each subtending 30° angle of rotation, and rotating either 1800 or 180 rpm. These rotational speeds permitted measurements over either approximately 2 or 20 milliseconds of cooling, excluding the partially closed intervals of the shutter cycle. The value of v_C for the 30° shutter was taken to be 0.96 from Table 11 of Appendix II.

Nonperiodic interruption was obtained with a solenoid-actuated flag-type shutter with approximately 6 milliseconds closure time placed near position D_1 of Figure 1.

In both cases, the oscilloscope was set for an appropriate sweep speed and triggered manually. The cooling rate of the sample, measured by the photocell through the 5545 A interference filter of F_2, was recorded on Polaroid film; the oscillograph trace was later measured on a two axis traveling microscope to obtain data for the desired time-temperature plot. Reflectance data for the sample were likewise obtained from the recorded oscilloscope traces. The oscilloscope deflections corresponding to the emitted radiance of the sample were converted into temperature values by placing the pyrometric arc at the sample position E in the furnace. This standard source of 3800°K spectral radiance temperature was used with appropriate neutral density filters to calibrate the photocell-oscilloscope combination for lower temperatures. The reflectance component was determined by relating the magnitude of the corresponding oscilloscope deflection with that for a water-cooled magnesium oxide coated surface (reflectance taken to be 0.98 at 5545 A) placed at sample position E.

5.1.6. Depth of Penetration of Cooling

The depth of material to which cooling penetrates with a semi-infinite body is measured approximately by:

$$\ell = \left(\frac{K\,t}{c\,\rho} \right)^{1/2} .$$

Since penetration depths characteristic of the experimental studies will be discussed along with the other experimental results, it will suffice here to point out that penetration depths for graphite at the temperatures concerned range from 0.1 mm or less with the 1800 rpm shutter to as much as one mm with the solenoid operated shutter.

5.1.7. Materials Used for Studies of Cooling

Several standard National Carbon Company grades of materials having typical properties shown in Table 7 were employed for this preliminary

Table 7. Physical Properties of Carbon and Graphite Materials Used in Studies of Cooling

Grade*	Base Material	Method of Forming	Bulk Density g/cc	Specific Resistance 10^{-4} ohm cm With Grain	Across Grain	Crystallinity of Material
ATJ	Petroleum Coke	Molded	1.73	11.0	14.5	Graphitic
CEP	Lampblack	"	1.55	48.0**		Nongraphitic
SPK	Petroleum Coke	Extruded	1.90	11.4	----	Graphitic
AGKSP	"	"	1.61	6.4	----	Highly graphitic
L113SP	Lampblack	"	1.45	64.0	----	Nongraphitic

* All National Carbon Company commercial grades

** Nearly isotropic

exploration of cooling behavior. Grade ATJ is a fine-grain molded graphite of relatively high density, conductivity and average anisotropy. Grade CEP is a fine-grain, almost isotropic, lampblack-base, molded graphite of relatively low density and low conductivity. Grades SPK, AGKSP and L113SP are extruded grades of spectroscopic purity. Grades SPK and AGKSP are graphite grades of spectroscopic purity. Grades SPK and AGKSP are graphite grades and Grade L113SP is made of lampblack-base filler materials. The lampblack-base materials show relatively high electrical resistivities.

Various geometries and sizes of samples were evaluated (see Section 5.1.8.). Figure 10 shows two sample arrangements employed: a) a simple cylinder; and b) a cylindrical central active portion surrounded by a concentric guard cylinder to reduce lateral heat losses.

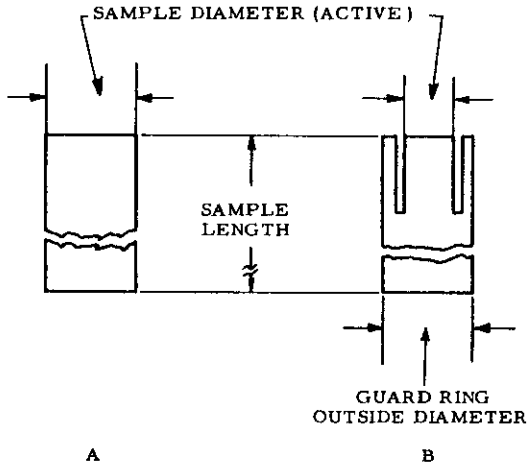

Figure 10. Sample Geometries for Cooling Studies

5.1.8. Experimental Results

Table 8 presents preliminary measurements of surface cooling and thermal conductivity of samples taken from the same material used for unpublished measurements by Doar and Pike on rectangular bar samples using a modification [23] of the Longmire method. These exploratory measurements were made to determine how the results by the two methods would compare. Samples were prepared with the grain orientations and the surface finishes described in Table 7.

Incident furnace irradiance and the fraction reflected by the sample were measured with a thermopile as described in Section 4.1.1. Bulk density of sample specimens were determined from their mass and bulk volume. Specific heat of the samples was assumed to be 0.52 cal/gram °K for the temperatures involved (near 2500°K).

Figure 11 shows oscillograph traces of the surface temperature of Grade ATJ graphite with 80-grit surface during cooling intervals for both nonperiodic and also 1800 rpm rotating shutters. The data from Figure 11 is shown in Figure 12 where surface temperature is plotted against square root of cooling time, measured from the middle of the shutter closing period.

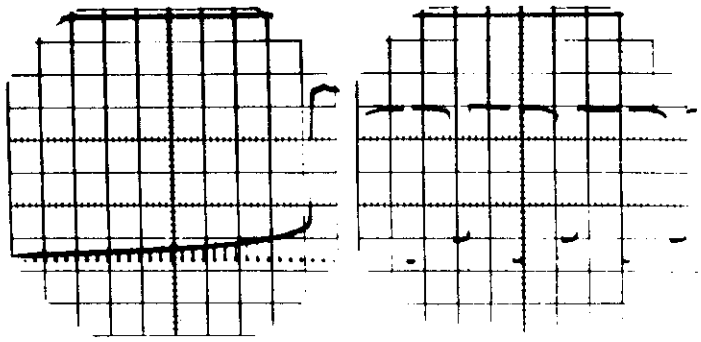

N-4336

A. Nonperiodic Shutter, Sweep Rate 50 Milliseconds Per Square

B. 1800 rpm Rotating Shutter, Sweep Rate 5 Milliseconds Per Square

Figure 11. Oscillograph Traces of Surface Cooling of Grade ATJ Graphite in Arc Image Furnace

The data for the nonperiodic shutter show excellent linearity except near the extremes. The data for the rotating shutter, although less well defined, show a short interval from which a linear slope can be determined; there is deviation at the beginning and end of the cooling interval due to reflected light from the incompletely closed shutter. Data obtained in a similar manner, shown in Table 8, reveals several significant features. First, the values of

Table 8. Thermal Conductivity of Carbon and Graphite Measured in Arc Image Furnace

Material*	Absorptance**	Bulk Density g/cc	Nonperiodic Shutter				1800 rpm Shutter				Measured by Rectangular Bar Method ††	
			Spectral† Reflectance	Radiance† Temp., °K	Thermal Conductivity Cal/cm sec /°K	Diffusivity k cm²/sec	Spectral† Reflectance	Radiance† Temp., °K	Thermal Conductivity Cal/cm sec /°K	Diffusivity k cm²/sec	Temp. °K	Thermal Conductivity Cal/cm sec /°K
A. Surface Prepared on 80-Grit Garnet Paper												
Grade ATJ – with grain	0.91	1.73	0.072	2568	0.100	0.111	0.070	2455	0.051	0.057	2000	----
Grade ATJ – across grain	0.91	1.73	0.070	2650	0.086	0.096	0.066	2547	0.032	0.036	2000	----
Grade CEP – ~ isotropic	0.925	1.55	0.048	2836	0.062	0.078	0.041	2753	0.046	0.058	2000	----
B. Surface Sandblasted												
Grade ATJ – with grain	0.91	1.73	0.064	2615	0.102	0.113	0.063	2473	0.093	0.103	2000	0.100
Grade ATJ – across grain	0.91	1.73	0.056	2625	0.099	0.110	0.055	2501	0.067	0.074	2000	0.074
Grade CEP ~ isotropic	0.925	1.55	0.040	2810	0.062	0.078	0.035	2748	0.041	0.052	2000	0.036

* Samples 0.19 in dia x 3/4 in lgth with guard ring 0.365 in O.D.; specific heat for all materials assumed 0.52 cal/gram °K; measurements are average of 2 or 3 samples.

** Total absorptance by sample of furnace irradiance, 8.62 watts per mm².

† Measured at 5545 A wavelength.

†† Measured by J. Doar, unpublished results using the Longmire method with a rectangular bar shape.

thermal conductivity obtained with the rotating shutter are significantly lower than with the nonperiodic shutter. Second, surface finish has no appreciable effect on thermal conductivity with the nonperiodic shutter; but when using the 1800 rpm rotating shutter, the 80-grit surface finish results in markedly lower thermal conductivity for the grade ATJ samples than does the sand-blasted surface. Both of these effects are attributed to the different properties of the material near the surface and the different depths of penetration of cooling involved with the two shutters, approximately one-tenth mm with the rotating shutter and one millimeter with the nonperiodic shutter. Table 8 also demonstrates that there is a fairly good correlation between the thermal conductivity values obtained from the arc image furnace and those obtained by the rectangular bar method. The thermal conductivity values from the rectangular bar method fall intermediate between those obtained by the two shutters with the arc image furnace. This observation may indicate some influence of surface properties with the rectangular bar samples, which were only one mm thick.

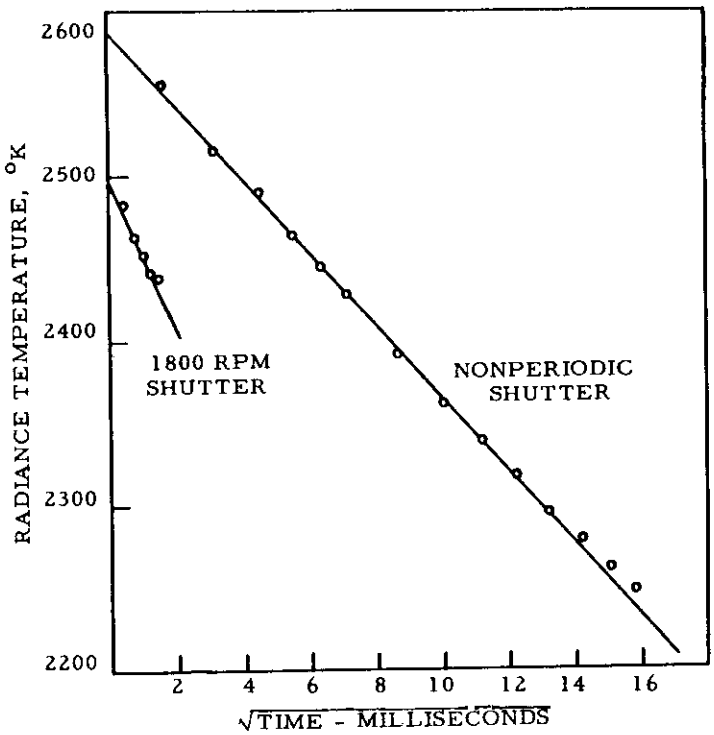

N-4365

Figure 12. Plot of Surface Temperature of Grade ATJ Graphite vs. Square Root of Time of Cooling

In view of the encouraging correlation between the values of thermal conductivity obtained by the arc image furnace and by the rectangular bar method, further tests were carried out to study the influence of sample geometry and size.

Part A of Table 9 describes cooling results obtained with five grades of graphite and three different sample sizes and shapes: one without guard ring

Table 9. Study of Effect of Sample Geometry on Calculated Thermal Conductivity Measured with Arc Image Furnace and Nonperiodic Shutter

Material*	Absorptance**	Bulk Density g/cc	Spectral† Reflectance	Radiance† Temp., °K	Thermal Conductivity Cal/sec cm °K	Spectral† Reflectance	Radiance† Temp., °K	Thermal Conductivity Cal/sec cm °K	Spectral† Reflectance	Radiance† Temp., °K	Thermal Conductivity Cal/sec cm °K
A. Active Sample Size → / Guard Ring Size →			0.365 in dia x 3/8 in lgth, No guard ring			0.19 in dia x 3/4 lgth, guard ring 0.365 in O.D.			0.346 in dia x 3/4 in lgth, guard ring 0.490 in O.D.		
Grade ATJ	0.91	1.73	0.077	2543	0.084	0.086	2709	0.077	0.062	2526	0.103
" CEP	0.925	1.55	0.063	2691	0.076	0.056	2870	0.069	0.040	2767	0.081
" SPK	0.91	1.90	0.062	2399	0.141	0.069	2539	0.129	0.050	2394	0.145
" AGKSP	0.90	1.61	0.070	2416	0.175	0.064	2568	0.131	0.040	2438	0.149
" L113SP	0.91	1.45	0.064	2709	0.064	0.054	2838	0.071	0.035	2743	0.074
B. Samples 0.19 in dia with 0.365 in O.D. guard ring			3/8 in lgth			3/4 in lgth			1-1/8 in lgth		
Grade AGKSP	0.90	1.61	0.074	2597	0.117	0.058	2583	0.127	0.038	2572	0.136
" CEP	0.925	1.55	0.062	2845	0.064	-----	----	-----	-----	----	-----
C. Samples 0.19 in dia with 0.365 in O.D. BN guard ring											
Grade AGKSP	0.90	1.61	0.069	2668	0.133	0.075	2694	0.122	-----	----	-----
CEP	0.925	1.55	0.046	2895	0.066	0.047	2897	0.067	-----	----	-----

* All samples had 80-grit surface finish; grades ATJ and CEP were molded and cut cross grain; grades SPK, AGKSP and L113SP were extruded and cut with grain; measurements are average of 2 or 3 samples.

** Total absorptance by samples of furnace irradiance, 8.62 watts per mm^2.

† Measured at 5545 A wavelength.

as shown in Figure 10A and two with guard rings as in Figure 10B. The sample without guard ring has approximately the same diameter as the outside diameter of the small guard ring and, also, approximately the active sample area inside the large guard ring. Table 9 indicates that except for the material of lowest conductivity, the smallest active diameter, 0.19 inch, gave smaller calculated thermal conductivity than the larger active diameter. It is believed that this differences results from lateral heat flow into the cooler outer portions of the larger diameter samples; this condition results in rapid decrease in axial heat flux below the surface and departure from one dimensional conduction assumed for the mathematical solution in Appendix II. This error appears to be reduced with the material of lower thermal conductivity.

The sample of smallest diameter with graphite guard ring was evaluated in 3/8, 3/4 and 1-1/8 inch lengths, as shown in Part B of Table 9. There is a small increase in calculated thermal conductivity with the longer specimens. Part C of Table 9 reports similar tests with a guard ring made from boron nitride material to test the effect of this low emissivity material as a radiation shield, but little difference was noted with the BN material. The guard ring geometry with smallest diameter and length was chosen for additional tests, although further tests would be desirable to make a choice of preferred length of specimen for tests with the nonperiodic shutter.

Table 10 reports tests run with graphite of high (Grade AGKSP) and low (Grade L113SP) thermal conductivity to study the effect of surface finish. A rotating shutter was run at 1800 and 180 rpm to evaluate the effect of increased time of cooling and depth of penetration using the same type of shutter. As before, the nonperiodic shutter was also used.

Part A of Table 10 gives results obtained on material with a surface finish prepared on 80-grit garnet paper. The most interesting feature is the very low values of thermal conductivity obtained with the 1800 rpm shutter for the Grade AGKSP graphite. The conductivity falls as low as 0.013 cal/sec cm°K which is only one-third to one-half the corresponding values for Grade ATJ graphite in Table 8. Data in Table 10A show that the tenfold higher time of cooling obtained with the 180 rpm shutter gave a much larger increase in the thermal conductivity of Grade AGKSP material than the Grade L113SP. In fact, the 1800 rpm shutter indicates that the more graphitic Grade AGKSP material has lower thermal conductivity near the surface than the Grade L113SP material, whereas the 180 rpm shutter indicates that the reverse is true for the underlying material. It is possible that a minor part of the indicated increase in conductivity with the 180 rpm shutter is not valid because the temperature change during the cooling period was enough to result in 10 to 15 per cent decrease in the radiation loss, a quantity assumed constant for the mathematical solution to the problem.

An effort was made to rerun the specimens of Table 10A with unaltered surface finish in order to check the observed results. Table 10B shows that this effort was only partially successful. There was an unexpected increase in reflectance and conductivity with the Grade AGKSP material but not so much with the Grade L113SP material. This change during the rerun may have been

Table 10. Study of Thermal Conductivity with Arc Image Furnace Using Different Shutters* and Surface Finishes

Material**	Absorptance†	1800 rpm Shutter			180 rpm Shutter			Nonperiodic Shutter		
		Spectral†† Reflectance	Radiance†† Temp., °K	Thermal Conductivity Cal/sec cm /°K	Spectral†† Reflectance	Radiance†† Temp., °K	Thermal Conductivity Cal/sec cm /°K	Spectral†† Reflectance	Radiance†† Temp., °K	Thermal Conductivity Cal/sec cm /°K
A. 80-Grit Surface Finish										
Grade AGKSP	0.90	0.056	2407	0.013	0.057	2374	0.101	-----	----	-----
" L113SP	0.91	0.052	2665	0.036	0.054	2611	0.065	-----	----	-----
B. Same Samples Re-run										
Grade AGKSP	0.90	0.064	2438	0.024	0.065	2402	0.150	0.067	2550	0.104
" L113SP	0.91	0.046	2672	0.054	0.053	2624	0.063	0.054	2779	0.043
C. Polished Surfaces										
Grade AGKSP	0.75	0.33	2373	0.021	0.29	2355	0.071	0.28	2516	0.103
" L113SP	0.72	0.25	2653	0.038	0.22	2616	0.048	0.14	2836	0.045
D. Broken Surfaces										
Grade AGKSP	0.90	0.052	2431	0.031	0.056	2377	0.116	0.055	2526	0.127
" L113SP	0.91	0.031	2653	0.038	0.034	2604	0.073	0.038	2753	0.072

* Times of cooling are approximately 2, 20 and 100 milliseconds respectively for the 1800 rpm, 180 rpm, and nonperiodic shutters.

** Samples 0.19 in dia x 3/8 in lgth with guard ring 0.365 in O.D.; material is extruded and samples were cut with grain; measurements are average for 2 or 3 samples.

† Total absorptance by samples of furnace irradiance, 8.62 watts per mm^2.

†† Measured at 5545 A wavelength.

due to high temperature vaporization or oxidation of some of the surface material, possibly due to incomplete protection from oxidation in the open end tube. Other studies have indicated good reproducibility of results on a given sample.

Table 10C presents results on polished surfaces. Again, a larger change was observed in conductivity for the two speeds of the rotating shutter with Grade AGKSP than Grade L113SP material. The same result is indicated by observation in Table 10D on broken surfaces, prepared in an effort to avoid mechanical polishing or abrasion of the surface.

The above results all indicate that mechanical polishing or abrasion of the surface results in markedly lower thermal conductivity for the material lying within ~ 0.1 mm of the surface than for the underlying material. That this effect is greatest with the most graphitic material (Grade AGKSP) and least with the least graphitic (Grade L113SP) can be explained on the basis that mechanical abrasion or polishing covers the surface and fills the voids with material oriented predominantly with its low thermal conductivity direction perpendicular to the surface, that is, turned at right angles to the low conductivity direction in the body of these extruded pieces. The loose bonding of such surface material would also result in low conductivity. The low anisotropy and crystallinity of the Grade L113SP material would be expected to result in less effect on the conductivity of the surface material.

5.2. Heating and Cooling as Affected by Surface Oxidation

Some studies on the effect of surface oxidation have given further insight into the effect of the surface condition on the heating and cooling of materials in the arc image furnace.

For these studies, the arc image furnace shown in Figure 1 was fitted with shutter S_1 at the intermediate focus shutter having 90° segments. A shutter having two 8 degree openings was used at the S_2 position. The test sample was viewed at 45° from the optical axis with an American Optical Company high temperature microscope. The resultant photographs were taken through the microscope objective by a 35 mm camera with its focus set at infinity. The surface could be photographed by emitted or emitted plus reflected light. The exposure time was governed by shutter S_2 rather than the camera shutter, especially for pictures taken by emitted light. Proper adjustment of the phase relationship between the two shutters rotating at 1800 rpm permitted observations of the surface by emitted light during cooling times up to 7 milliseconds after complete closure of the shutter or by emitted plus reflected light for other parts of the cycle.

Samples of nominal 3/8 inch diameter and length were used. The exposed surface was prepared by scoring the circumference of the parent rod with a knife and then breaking the sample from it. Samples were obtained in this manner free from mechanical surface working except for that involved in the fracture process. These samples were protected from oxidation during heating by mounting them in an open-ended tube surrounded by flowing argon. Oxidized samples of the same dimensions were prepared by interrupting the

argon flow for a few minutes and then restoring it to preserve the surface for further study.

Figure 13 shows photographs taken with the High Temperature Microscope using "National" Grade AGKSP spectroscopic graphite. Exposure conditions were not strictly comparable throughout the two series – in both cases the reflected light was several times greater than the emitted light.

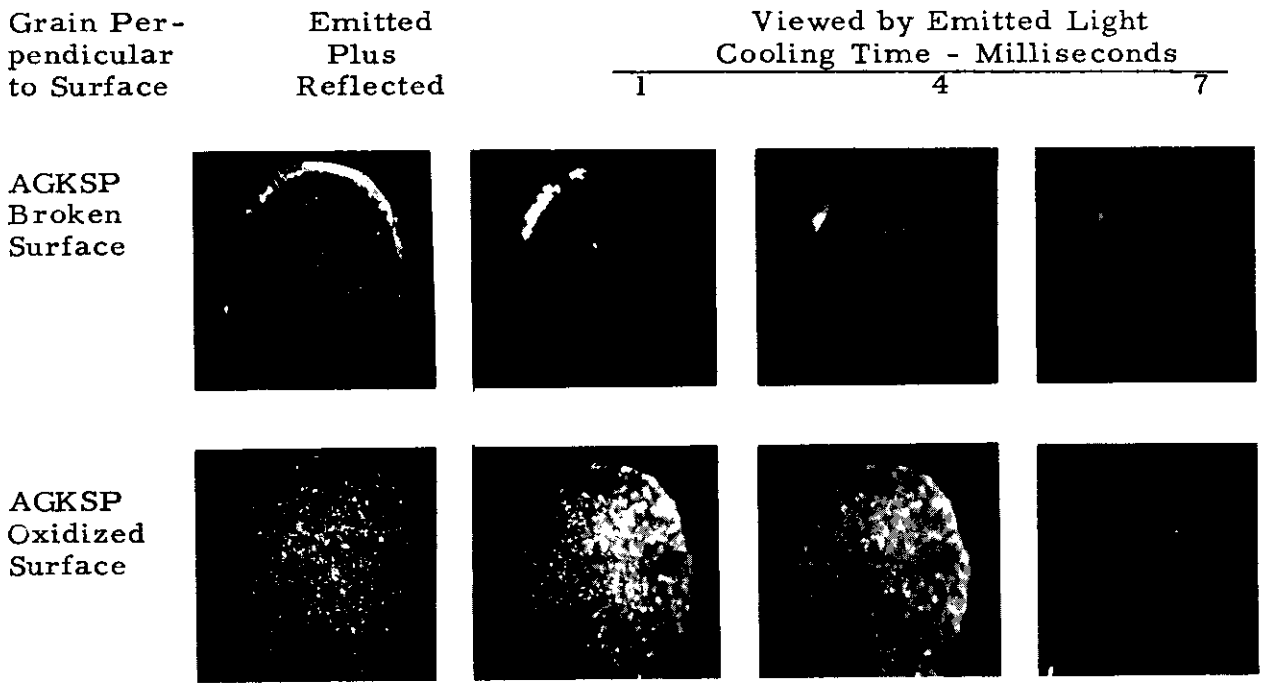

N-940

Figure 13. Cooling of Graphite Samples in Argon Atmosphere After Interruption of Arc Image Furnace Radiation - Magnification - 3 X

Figure 13 shows two series of views of samples made with the sample held in an argon atmosphere. The first series represents a broken surface of AGKSP grade of spectroscopic graphite. The first view in each series included reflected light and delineated the visual surface detail which is almost lacking in the emitted light. The few bright spots observed 1 millisecond after the shutter interruption were observed to cool markedly faster than the background in a few milliseconds. Analysis indicates that these were in fact poorly attached areas which in some cases cooled below the substrate temperature during the 7 millisecond time interval.

The second series of Figure 13 is similar except that the surface of the AGKSP sample was allowed to oxidize in air for a few minutes before restoring

the argon atmosphere and taking the photographs. In this series, prior oxidation produced a marked increase in the number and intensity of these brightly glowing spots which, as before, cooled more rapidly than the substrate.

The conclusion that the brightly glowing and rapidly cooling areas of Figure 13 are poorly connected thermally to the substrate is borne out by photomicrographic cross-sections of the materials as shown in Figure 14. After exposure in the arc image furnace, the samples were impregnated with epoxy resin and imbedded in Lucite before cross-sectioning and polishing. In each case, the furnace-exposed face of the sample is at the top of the picture. Increased isolation of individual coke particles of the AGKSP material is clearly evident near the exposed surface after oxidation (see Figure 14). It is understandable that these isolated particles would become hotter and cool faster than the substrate.

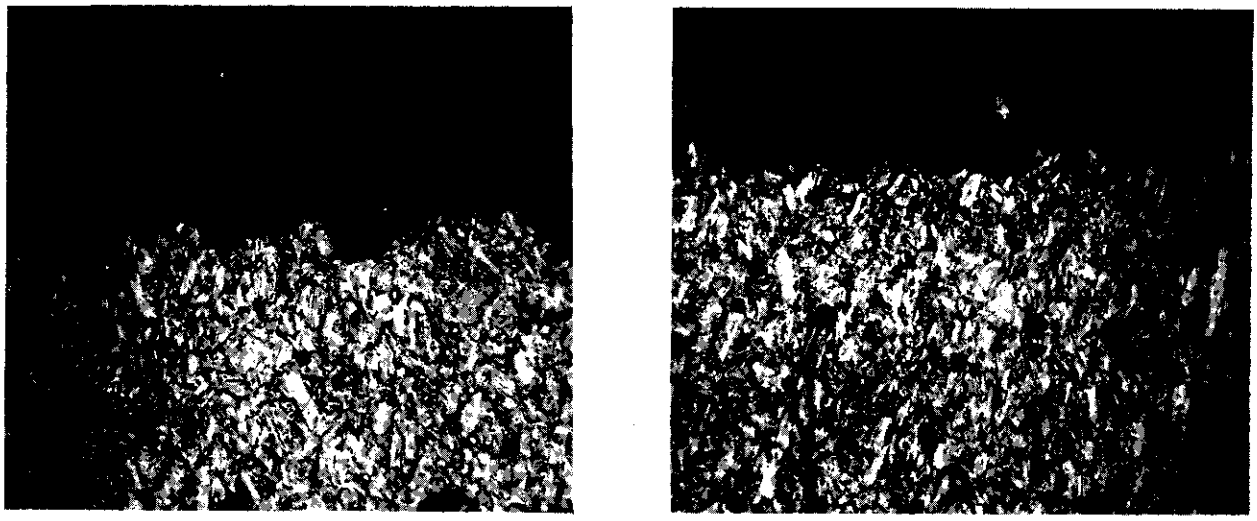

N-985

Figure 14. Photomicrographs of Cross-Sections of Grade AGKSP Graphite after Exposure in Carbon Arc Image Furnace - Magnification 25 X

Rough calculation of the thickness of the thermally insulated layer on the oxidized AGKSP material obtained from its cooling rate indicates a minimum thickness of 50-65 microns, which is well within the range of particle sizes observed near the exposed surface of Figure 14.

APPENDIXES I THROUGH III

APPENDIX I

APPROXIMATE CALCULATION OF REFLECTANCE AND POLARIZATION OF LIGHT REFLECTED FROM GRAPHITE AT 45° ANGLE OF INCIDENCE

McCartney and Ergun[21] have shown that single crystal graphite is a negative uniaxial crystal which has an optic axis perpendicular to the layer planes and has principal indices of refraction n = 2.15 and 2.00 at 5460 A wavelength and corresponding absorption indices k = 0.66 and 0.01. These quantities refer respectively to the electric vector parallel and perpendicular to the layer planes. Reflection formulas have been developed for highly absorbing homogeneous materials (metals) and for anisotropic nonabsorbing materials (dielectrics) but not for a highly absorbing, anisotropic body such as crystalline graphite at other than normal incidence.

The following formulas[24] are approximately valid for the reflectance from isotropic absorbing materials when $n^2 + n^2 k^2 >> 1$:

$$r_{\parallel} = \frac{\left(n - \frac{1}{\cos\varphi}\right)^2 + n^2 k^2}{\left(n + \frac{1}{\cos\varphi}\right)^2 + n^2 k^2} \qquad (1)$$

$$r_{\perp} = \frac{(n - \cos\varphi)^2 + n^2 k^2}{(n + \cos\varphi)^2 + n^2 k^2} , \qquad (2)$$

where φ is the angle of incidence and $r_{\parallel}$ and $r_{\perp}$ measure the reflectance for radiation polarized with the electric vector respectively parallel and perpendicular to the plane of incidence. If we assume that these formulas are also applicable to the anisotropic uniaxial graphite crystal, then certain conclusions can be drawn.

Figure 15 shows three cases of special interest. The optic axis is perpendicular to the layer planes. Case 1 describes the case where the layer planes are parallel to the surface of the graphite crystal. The instances where the layer planes are perpendicular to the surface are covered by Cases 2 and 3 respectively for the layer planes parallel and perpendicular to the plane of incidence. Figure 15 identifies separately the two orientations of polarization with respect to the plane of incidence. The refracted rays remain in the plane of incidence for all three cases.

Figure 15 shows the index of refraction and angle of refraction obtained from McCartney and Ergun's data[21] for each of the six combinations and indicates approximate directions of vibration for the refracted rays. The

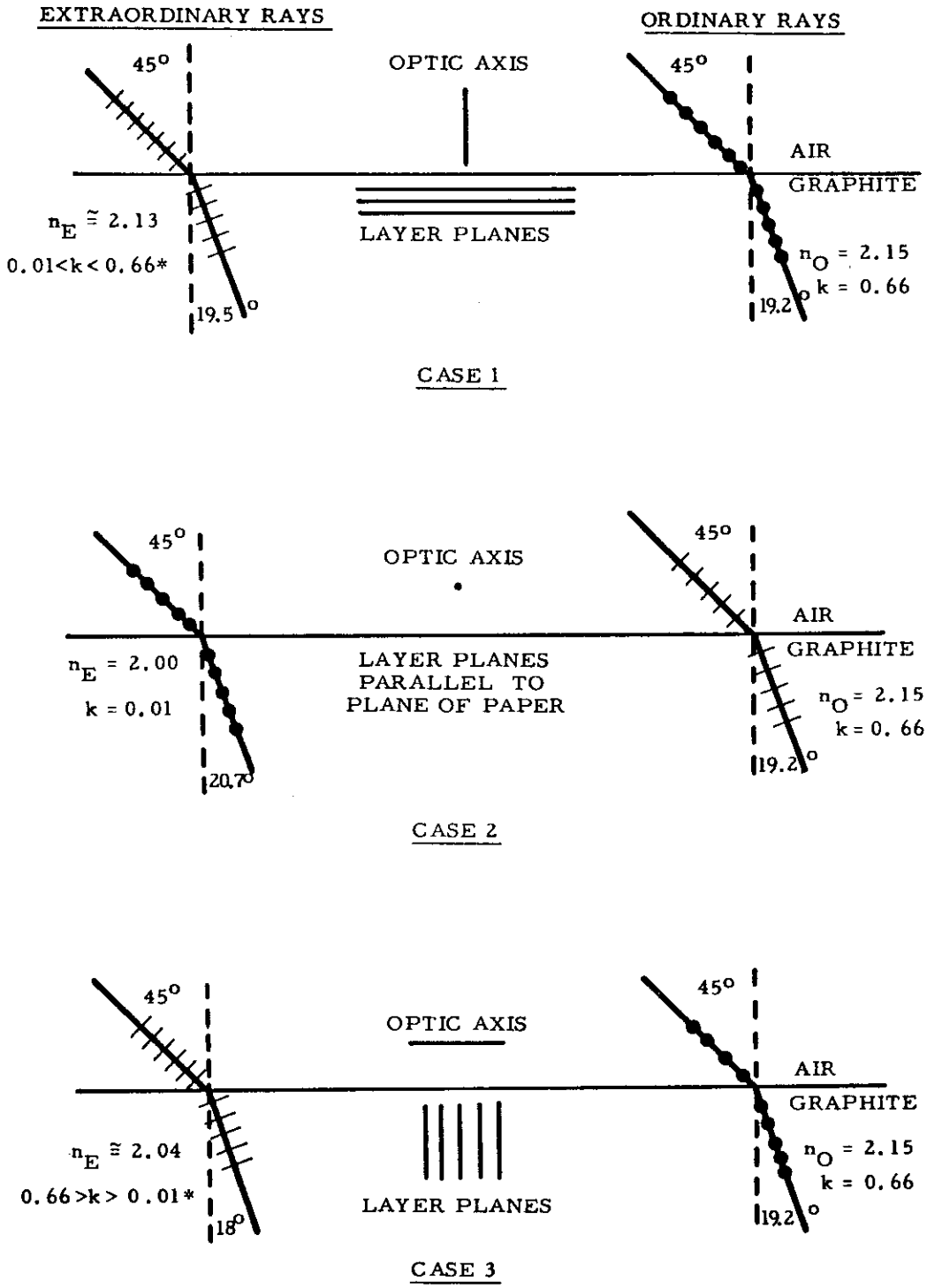

N-4366

Figure 15. Refraction of Rays in Single Crystal Graphite with 45° Angle of Incidence

absorption indices are unambiguous in all but two instances, the extraordinary rays for Cases 1 and 3. Here, the electric vector is neither parallel or perpendicular to the layer planes but lies in an intermediate direction. However, since the electric vector in the refracted beam is inclined less than 20° from the layer planes in Case 1, it appears reasonable that the component of the electric vector along the layer planes would produce considerable conductivity, absorption, and resultant reflection. Similarly, the electric vector in the refracted beam for Case 3 is inclined 18° from the optic axis and its major component along this direction should result in small conductivity, absorption and reflection. Accordingly, the preferred ends of the ranges of possible values of k for Cases 1 and 3 are starred (*) in Figure 15 and in subsequent calculations.

The values of n and k shown in Figure 15 have been substituted in Equations (1) and (2) to calculate the reflectance and polarization for the cases of Figure 15. The average reflectance for unpolarized light, given by $r = \frac{r_\perp + r_\parallel}{2}$, and the polarization given by $P = \frac{r_\perp - r_\parallel}{r_\perp + r_\parallel}$, have already been listed in Table 5 in Section 4.3.

APPENDIX II

PERIODIC SURFACE HEATING OF A SEMI-INFINITE BODY

Application of the carbon arc image furnace to the study of the properties of materials requires a knowledge of their cooling and heating behavior under various environments of thermal radiation, conduction and convection. A specific problem of direct interest is the variation of surface temperature of a material body placed at the focus of a carbon arc image furnace with the furnace irradiation interrupted periodically by a rotating shutter. The radiant energy falling on an opaque material is partly reflected and partly absorbed. The absorbed energy is converted to heat which is dissipated by thermal radiation, conduction, and convection. The resultant temperature of the surface material is a complicated balance between all of these components.

A regular body such as a circular cylinder having a plane, symmetrically irradiated surface offers simplifications which can be treated mathematically. In such cases, the surface temperature of a homogeneous material is observed to be essentially uniform over a substantial area of the exposed end. There can be no lateral heat conduction in such regions of uniform temperature and the problem reduces to one-dimensional heat conduction. During transient intervals that are sufficiently short, the body can be considered as semi-infinite and the corresponding mathematical solutions can be applied.

The problem of the temperature variation of the surface of a semi-infinite body subjected to a periodic heat flux has been solved by Jaeger [25] for the case of one-dimensional heat flow normal to the surface. The solution which is discussed below involves integrals which must be evaluated numerically. Such an evaluation has been made on a Royal Precision LGP-30 computing machine at this laboratory and the solution is included in this Appendix.

Carslaw and Jaeger show [25] that for a semi-infinite solid of thermal conductivity K, specific heat c, and density ρ, initially at zero temperature throughout and subjected at time zero to a continuing series of periodic rectangular pulses of heat flux H_o applied at the surface for the fraction a of the total time, the surface temperature T_s after a large number of periods and large values of time t may be expressed by:

$$T_s = 2 H_o a \left(\frac{t}{\pi K c \rho}\right)^{1/2} + T_p . \qquad (1)$$

The first part of Equation (1) gives a slowly rising surface temperature which is exactly equivalent to that of a semi-infinite body receiving the average integrated flux a H_o. The second part of Equation (1), T_p, gives the periodic portion of the temperature variation within the individual heating and cooling portions of the cycles as described below. Letting τ equal the pulse periodicity (heating plus cooling interval) and $b\tau$ the time interval after the

beginning of a heating period, the periodic temperature variation, T_p, is given during a heating interval by:

$$T_p = 2 H_o \left(\frac{\tau}{\pi K c \rho}\right)^{1/2} \left[(1-a) b^{1/2} - \pi^{-1/2} I(a, b)\right] \text{ for } 0 \leq b \leq a \ , \qquad (2)$$

and during a cooling interval by:

$$T_p = 2 H_o \left(\frac{\tau}{\pi K c \rho}\right)^{1/2} \left[(1-a) b^{1/2} - (b-a)^{1/2} - \pi^{-1/2} I(a, b)\right] \text{ for } a \leq b \leq 1, \qquad (3)$$

where

$$I(a, b) = \int_o^\infty \frac{e^{-b\xi^2}\left[(1-a)e^{-\xi^2} - e^{-(1-a)\xi^2} + a\right] d\xi}{\xi^2 (1 - e^{-\xi^2})} \qquad (4)$$

Equation (2) describes the temperature variation during a heating interval, $0 \leq b\tau \leq a\tau$, and Equation (3) that during a cooling interval $a\tau < b\tau < \tau$. Temperature maxima will occur at b = a and minima at b = 0 and 1. Substituting the appropriate values of a and b and measuring the changes in temperature from the beginning of a heating or cooling cycle, we obtain for the heating portion, $0 \leq b \leq a$,

$$\Delta T_H = \left[2 H_o \left\{\frac{b\tau}{\pi K c \rho}\right\}^{1/2}\right] b^{-1/2} \left[(1-a) b^{1/2} - \pi^{-1/2} \left\{I(a, b) - I(a, o)\right\}\right] , \qquad (5)$$

and for the cooling portion, $a \leq b \leq 1$,

$$\Delta T_C = \left[2 H_o \left\{\frac{(b-a)\tau}{\pi K c \rho}\right\}^{1/2}\right] (b-a)^{-1/2} \left[(1-a)(b^{1/2} - a^{1/2}) - (b-a)^{1/2} - \pi^{-1/2} \left\{I(a, b) - I(a, a)\right\}\right] . \qquad (6)$$

It will be noted that the first factor (in brackets) in Equation (5) has a square root of time dependence and represents the nonperiodic change in surface temperature over the same length of time $b\tau$ for a semi-infinite body initially at uniform temperature, subjected to addition of the same flux H_o. The remaining two factors in Equation 5 show the departure of the periodic heating from the nonperiodic heating relation. Similarly, the first factor (in brackets) in Equation (6) represents the nonperiodic change in temperature over the same length of time $(b-a)\tau$ for a semi-infinite body initially at uniform temperature, subjected to addition of the same flux H_o and, again, the remaining two factors measure the departure from the nonperiodic heating relation. Equation (6) represents cooling because, as will be shown, ΔT_C is negative.

The last two factors in Equation (5) and (6),

$$v_H = b^{-1/2}\left[(1-a)\,b^{1/2} - \pi^{-1/2}\left\{I(a,b) - I(a,o)\right\}\right] \quad , \qquad (7)$$

and

$$v_C = (b-a)^{-1/2}\left[(1-a)(b^{1/2} - a^{1/2}) - (b-a)^{1/2} - \pi^{-1/2}\left\{I(a,b) - I(a,a)\right\}\right] \quad , \qquad (8)$$

represent the ratio of the periodic to the nonperiodic heating relations described above. Equations (7) and (8), which were programmed and computed on a LGP-30 computing machine, are shown in Table 11 and Figure 16. It was unnecessary to compute $v_H(a, b)$ and $v_C(a, b)$ for values of $a > 0.5$. Because of the symmetry of the expressions, the values of v_H and v_C for b and a are exactly the same as the negative of those respectively for v_C and v_H with (b-a) substituted for b and (1-a) substituted for a. Therefore, as an example, the heating and cooling curves for a = 0.9 are identical respectively to the negative of the cooling and heating curves for a = 0.1.

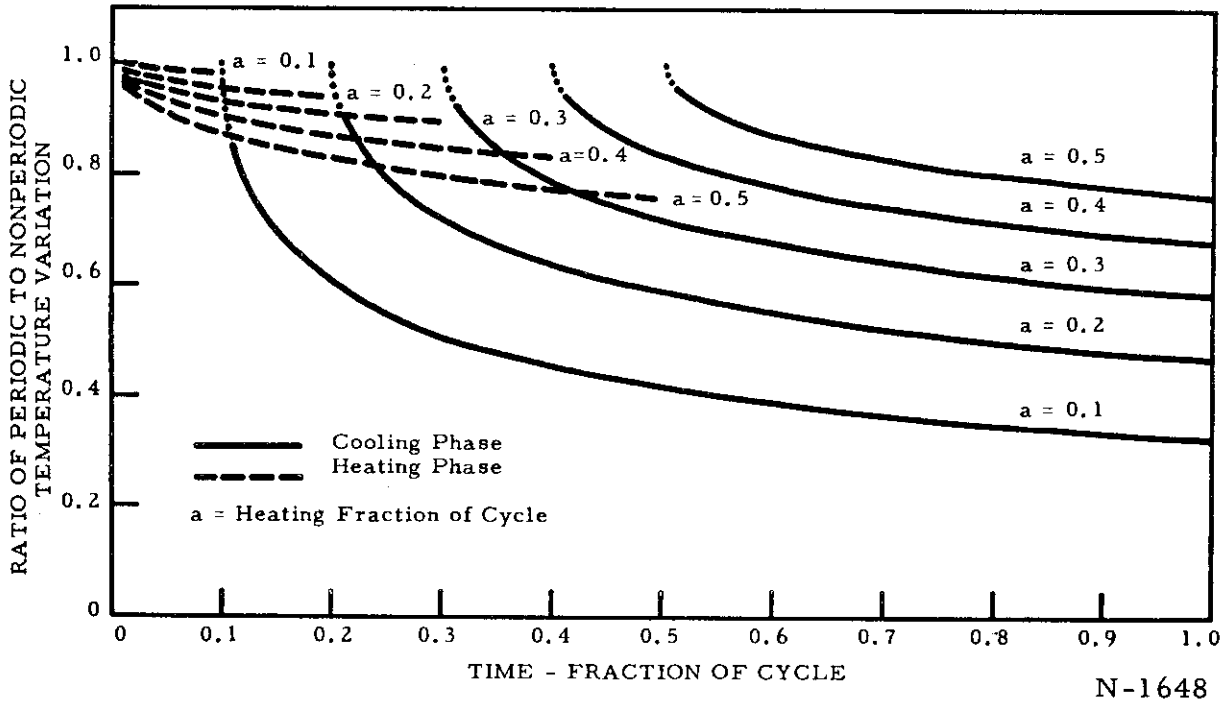

Figure 16. Surface Temperature Variation of Semi-Infinite Body During Periodic Heating and Cooling Compared to Nonperiodic Case

Figure 16 shows that for small values of a, that is, for cycles in which the heating portion is short compared to the cooling interval, then the heating portion approaches closely that of the nonperiodic heating, but the cooling

Table 11. Heating and Cooling Factors from Equations (7) and (8)

a=0.10			a=0.20			a=0.30		
b	v_H	$-v_C$	b	v_H	$-v_C$	b	v_H	$-v_C$
0.00	1.0000		0.00	1.0000		0.00	1.0000	
0.01	0.9932		0.01	0.9858		0.01	0.9776	
0.02	0.9905		0.02	0.9801		0.02	0.9685	
0.03	0.9884		0.03	0.9757		0.03	0.9616	
0.04	0.9866		0.04	0.9720		0.04	0.9559	
0.05	0.9851		0.05	0.9688		0.05	0.9509	
0.06	0.9837		0.06	0.9660		0.06	0.9465	
0.07	0.9825		0.07	0.9635		0.07	0.9424	
0.08	0.9814		0.08	0.9611		0.08	0.9394	
0.09	0.9803		0.09	0.9589		0.09	0.9353	
0.10	0.9793	1.0000	0.10	0.9568		0.10	0.9321	
0.11		0.8519	0.20	0.9413	1.0000	0.20	0.9079	
0.12		0.7954	0.21		0.9017	0.30	0.8913	1.0000
0.13		0.7549	0.22		0.8628	0.31		0.9271
0.14		0.7227	0.23		0.8340	0.32		0.8979
0.15		0.6960	0.24		0.8106	0.33		0.8760
0.16		0.6731	0.25		0.7907	0.34		0.8581
0.17		0.6531	0.26		0.7733	0.35		0.8427
0.18		0.6354	0.27		0.7578	0.36		0.8291
0.19		0.6194	0.28		0.7439	0.37		0.8170
0.20		0.6050	0.29		0.7311	0.38		0.8059
0.30		0.5087	0.30		0.7194	0.39		0.7957
0.40		0.4540	0.40		0.6369	0.40		0.7863
0.50		0.4172	0.50		0.5864	0.50		0.7182
0.60		0.3902	0.60		0.5509	0.60		0.6748
0.70		0.3692	0.70		0.5240	0.70		0.6434
0.80		0.3523	0.80		0.5027	0.80		0.6191
0.90		0.3383	0.90		0.4853	0.90		0.5997
1.00		0.3264	1.00		0.4706	1.00		0.5835
b-a	$-v_C$	v_H	b-a	$-v_C$	v_H	b-a	$-v_C$	v_H
a=0.90			a=0.80			a=0.70		

a=0.40			a=0.50			a=5/6		
b	v_H	$-v_C$	b	v_H	$-v_C$	b	v_H	$-v_C$
0.00	1.0000		0.00	1.0000		0.00	1.0000	
0.01	0.9683		0.01	0.9575		0.01	0.8895	
0.02	0.9555		0.02	0.9403		0.02	0.8461	
0.03	0.9457		0.03	0.9273		0.03	0.8142	
0.04	0.9377		0.04	0.9165		0.04	0.7884	
0.05	0.9307		0.05	0.9072		0.05	0.7666	
0.06	0.9244		0.06	0.8990		0.06	0.7476	
0.07	0.9188		0.07	0.8915		0.07	0.7308	
0.08	0.9136		0.08	0.8846		0.08	0.7157	
0.09	0.9088		0.09	0.8783		0.09	0.7019	
0.10	0.9043		0.10	0.8724		0.10	0.6894	
0.20	0.8708		0.20	0.8286		0.20	0.6019	
0.30	0.8480		0.30	0.7993		0.30	0.5494	
0.40	0.8309	1.0000	0.40	0.7775		0.40	0.5129	
0.41		0.9443	0.50	0.7602	1.0000	0.50	0.4855	
0.42		0.9218	0.51		0.9575	0.60	0.4639	
0.43		0.9049	0.52		0.9403	0.70	0.4464	
0.44		0.8910	0.53		0.9273	0.80	0.4317	
0.45		0.8790	0.54		0.9165	5/6	0.4273	1.0000
0.46		0.8683	0.55		0.9072	0.84		0.9905
0.47		0.8587	0.56		0.8990	0.85		0.9850
0.48		0.8500	0.57		0.8915	0.86		0.9811
0.49		0.8419	0.58		0.8846	0.87		0.9780
0.50		0.8344	0.59		0.8783	0.88		0.9753
0.60		0.7791	0.60		0.8724	0.89		0.9729
0.70		0.7429	0.70		0.8286	0.90		0.9707
0.80		0.7162	0.80		0.7993	0.91		0.9687
0.90		0.6954	0.90		0.7775	0.92		0.9668
1.00		0.6784	1.00		0.7602	0.93		0.9651
						1.00		0.9554
b-a	$-v_C$	v_H	b-a	$-v_C$	v_H	b-a	$-v_C$	v_H
a=0.60			a=0.50			a=1/6		

Note—All values of b>1 are same as b-1.

curve differs markedly and for a = 0.1, falls as low as 0.33 of the nonperiodic value. When a is increased to 0.5 (equal heating and cooling phases), the periodic heating and cooling curves become identical and are below the nonperiodic case, as low as 0.76 at the extremes. It can be shown that all of the curves in Figure 16 have a value of one at the beginning of each phase, indicating that the initial temperature variation at the start of a heating or cooling phase is exactly that of the nonperiodic case.

It must be emphasized that these periodic solutions are valid only for those cases where the temperature variations during heating or cooling are small enough to leave the total rate of heat gain or loss at the surface unchanged. In practice, this condition can be sufficiently approximated by making the frequency of the heating sufficiently large.

The application of these formulas to the study of thermal conductivity is shown in Section 5.1.2.

APPENDIX III

NONPERIODIC COOLING OF SEMI-INFINITE BODY

Appendix II describes the case of periodic heating and cooling of a semi-infinite solid; another problem directly related to image furnace studies is the nonperiodic cooling of a heated material after interruption of the furnace radiation. After sufficiently long exposure of the material to furnace radiation, the irradiated surface attains a steady state balance between absorbed radiation and the losses due to convection, conduction and radiation. Since, immediately after interruption of the furnace radiation the various losses remain the same as they were immediately before the interruption, their sum at this time is equal to the total absorbed radiation. These losses along with the material properties control the cooling rate of the surface after interruption of the furnace radiation.

Appendix II explains that when the cooling time is sufficiently short, the problem can often be considered equivalent to the one-dimensional cooling of a semi-infinite body. Figure 17 shows a problem which has been considered, namely, a semi-infinite solid has a constant thermal gradient throughout at time $t = 0$, but is assumed to lose energy at $x = 0$ according to Newton's Law of Cooling after $t = 0$.

The equation of heat conduction is:

$$\frac{\partial T}{\partial t} = \frac{K}{c\rho} \frac{\partial^2 T}{\partial x^2} \quad (0 < x < \infty) \tag{1}$$

and the boundary conditions are:

$$K\frac{\partial T}{\partial x} = H(T - T_s) \quad \text{at } x = 0 \quad , \tag{2}$$

$$T = T_o - \frac{F_o\, x}{K} \quad \text{at } t = 0 \tag{3}$$

$$(T_o = T \text{ at } x = 0 \text{ and } t = 0) \quad , \tag{4}$$

where K, c and ρ are the thermal conductivity, specific heat, and density of the solid. $T = T(x, t)$ is the temperature in the solid. T_s is the temperature of the surroundings and H the cooling constant involved in Newton's Law of Cooling expressed in Equation (2). F_o is the conducted flux associated with the constant thermal gradient at $t = 0$ and is directed into the body.

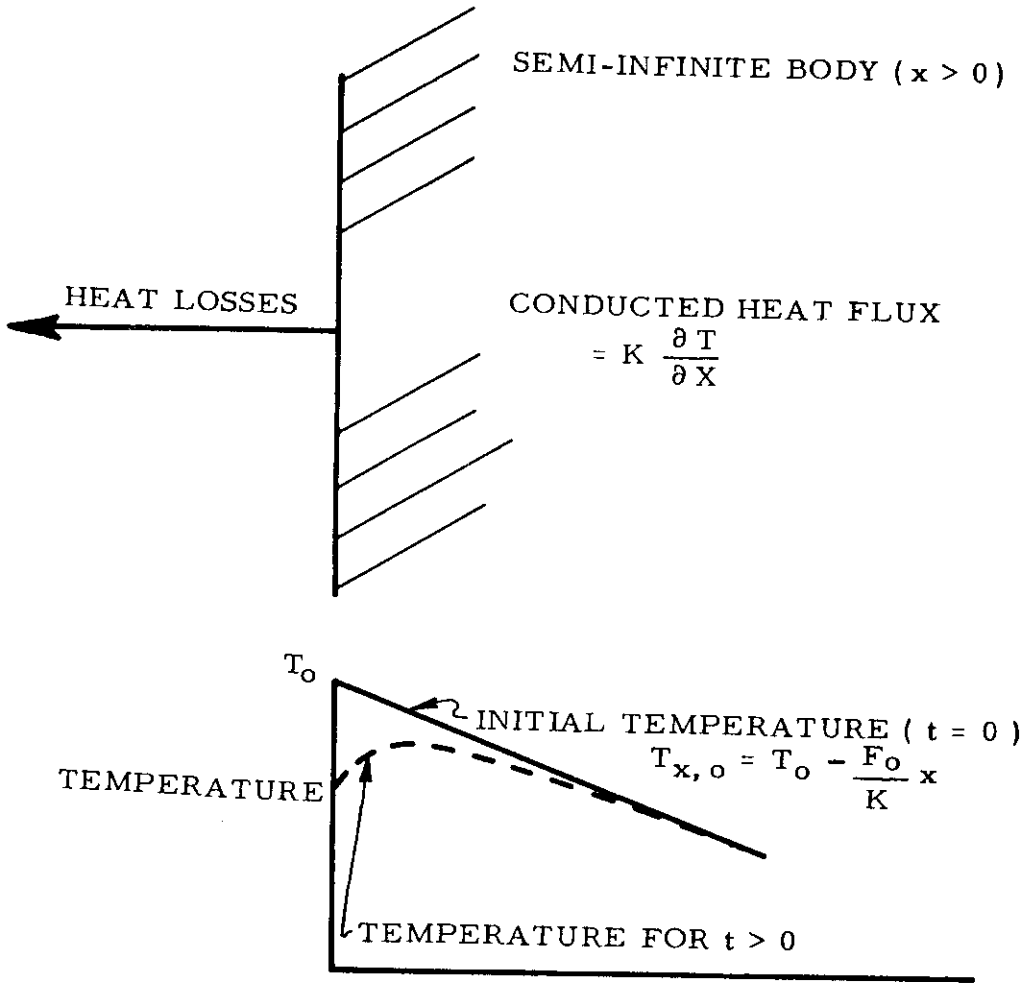

Figure 17. Semi-Infinite Body with Initially Constant Thermal Gradient

The solution to these equations,(*) readily obtained from Laplace Transforms, is as follows:

$$\Delta T\,(x,t) = T\,(x,0) - T\,(x,t)$$

$$= \frac{(R_o + F_o)}{H}\left[\operatorname{erfc}\left(\frac{x}{2\sqrt{kt}}\right) - \left(e^{hx + kth^2}\right)\operatorname{erfc}\left(\frac{x}{2\sqrt{kt}} + h\sqrt{kt}\right)\right] \qquad (5)$$

where $R_o = H(T_o - T_s)$ = surface losses at $t = 0$, $h = \frac{H}{K}$, and $k = \frac{K}{c\rho}$.

For $x = 0$ and $h\sqrt{kt} < 1$, Equation (5) can be expressed, approximately, as:

$$\Delta T\,(0,t) = \frac{(R_o + F_o)}{Kh}\left[2h\left(\frac{kt}{\pi}\right)^{1/2} - h^2 kt\right] . \qquad (6)$$

For $h\sqrt{kt} << 1$, Equation (6) reduces to

$$\Delta T\,(0,t) = 2\,(R_o + F_o)\left(\frac{t}{\pi K c \rho}\right)^{1/2} . \qquad (7)$$

Equation (7) is identical to the solution for the variation of surface temperature of a semi-infinite solid, initially at uniform temperature, but subjected to withdrawal of constant heat flux $(R_o + F_o)$ after $t = 0$. In other words, the presence of the initial thermally conducted flux F_o in the solid does not change the functional form of the variation of surface temperature with time but affects only the magnitude.

The accuracy with which the square root of time dependence of Equation 7 is followed is determined by the ratio of the second to the first term in Equation 6, that is, $h\,(\pi kt)^{1/2}/2 = H\,(\pi kt)^{1/2}/2\,K$. Substituting approximate values for the physical properties of graphite and realizing that the surface losses are mostly thermal radiation, it can readily be shown that the departures from the square root relationship of Equation (7) are no more than a few per cent over the temperature range 2000 to 3000°K for cooling times of some tens of milliseconds.

The application of Equation (7) to the determination of the thermal conductivity of graphite is discussed in Section 5.1.3. of this report.

(*) The authors are indebted to John N. Pike for the solution to this problem.

REFERENCES

1. M. R. Null and W. W. Lozier, Rev. Sci. Inst. 29, 163 (1958).

2. WADC Technical Report 59-789, Development of Graphite and Graphite-Base Multicomponent Materials for High Temperature Service, by W. W. Lozier.

3. ASTM Method D 986-50.

4. F. Benford, Gwen P. Lloyd and Sally Schwarz, J. Opt. Soc. Am. 38, 445 (1948).

5. W. E. Knowles Middleton and C. L. Sanders, J. Opt. Soc. Am. 41, 419 (1951).

6. C. L. Sanders and W. E. Knowles Middleton, J. Opt. Soc. Am. 43, 58 (1953).

7. M. R. Null and W. W. Lozier, J. Opt. Soc. Am. 52, 1156 (1962).

8. M. R. Null and W. W. Lozier, J. Soc. Mot. Pict. TV Engrs. 68, 80 (1959).

9. J. D. Plunkett and W. D. Kingery, Proceedings of the Fourth Conference on Carbon (Pergamon Press, New York, 1960), pp. 457-472.

10. H. T. Betz, O. H. Olson, B. D. Schurin and J. C. Morris, WADC Technical Report 56-222, Part I (1956).

11. J. T. McCartney and S. Ergun, Fuel 37, 272 (1958).

12. M. R. Null and W. W. Lozier, "Measurement of Reflectance and Emissivity at High Temperature with a Carbon Arc Image Furnace," presented at the Symposium on Measurement of Thermal Radiation Properties of Solids in Dayton, Ohio, on September 5-7, 1962. See also Section 4.2. of this report.

13. A. F. Grenis and A. P. Levitt, Watertown Arsenal Laboratories Technical Report Nos. WAL TR 397.1/2, November (1959) and WAL TR 851.2/1, May (1962).

14. R. J. Thorn and O. C. Simpson, J. Appl. Phys. 24, 633 (1953).

15. K. Warmuth, Wiss. Veroff. Siemens-Konz. 7, 307 (1928).

16. J. Euler, Am. Physik (6) 11, 203 (1953).

17. J. Euler, Am. Physik (6) 14, 145 (1954).

18. J. Euler, Ann. Physik (6) 18, 345 (1956).

19. J. Euler, Sitzber. Heidelberg Akad. Wiss. 1956/57, 4 Abh., p. 418.

20. W. W. Lozier and M. B. Manofsky, in Mechanical Properties of Engineering Ceramics, edited by W. Wurth Kriegel and Hayne Palmour III, (Interscience Publishers, New York, 1961), pp. 451-473.

21. J. T. McCartney and S. Ergun, Fuel 37:272-281 (1958).

22. G. Rupprecht, D. Ginsberg and J. Leslie, Jour. Opt. Soc. Am. 52, 665 (1962).

23. J. F. Doar and J. N. Pike, Proceedings of the Fifth Conference on Carbon, (Pergamon Press, New York, 1963), Vol. 2, pp. 311-317.

24. R. W. Ditchburn, Light (Blackie & Son Limited, London and Glasgow, 1953), p. 444; see also F. A. Jenkins and H. E. White, Fundamentals of Physical Optics, First Edition (McGraw-Hill Book Company, Inc., New York and London, 1937), p. 400.

25. H. S. Carslaw and J. C. Jaeger, 2nd Edition, "Conduction of Heat in Solids," Oxford University Press (1959), pp. 400-402. See also J.C. Jaeger, Quart. Appl. Math. 11, 132-137 (1953).